Oahu Hawaiian Hoary Bat
Occupancy and Distribution Study

Final Report

Prepared for:

Hawaii Endangered Species Research Committee

Prepared by:

Joel Thompson and Leigh Ann Starcevich

Western EcoSystems Technology, Inc.
2725 Northwest Walnut Boulevard
Corvallis, Oregon 97330

July 18, 2022

EXECUTIVE SUMMARY

In response to a request for proposals issued by Hawaii's Endangered Species Recovery Committee (ESRC) in 2016, Western EcoSystems Technology, Inc. (WEST) developed a five-year study proposal to assess Hawaiian hoary bat (HAHOBA) distribution and occupancy across the island of Oahu. The study was developed to allow for island-wide inference and used an equiprobable generalized random tessellation stratified sample of grid cells for the placement of acoustic bat detectors across Oahu.

Field data collection spanned a roughly four-year period, beginning in late spring 2017 and concluding in early fall 2021. Wildlife Acoustics Song Meter SM4Bat (SM4) full spectrum bat detectors were deployed for all data collection conducted by WEST. Acoustic detectors were deployed within selected grid cells with microphones placed approximately 10 feet (three meters) above ground. Detectors were left in the field year round at the location of original placement and programmed to record data from approximately one hour prior to sunset to approximately one hour after sunrise. Detectors were visited on a regular basis to download data and assess functionality. Acoustic recordings were processed with the Kaleidoscope Pro 5 software package (Wildlife Acoustics) to remove noise (i.e., non-bat) files and convert the full-spectrum call files to zero-cross files. A bat biologist with training and experience in acoustic bat call analysis then reviewed all call files identified as bats to ensure they contained a minimum of two distinct pulses and to confirm the recording was consistent with that of a HAHOBA.

Acoustic detection data were examined using a dynamic occupancy analysis for correlated detections to obtain estimates of occupancy and detection rates. Occupancy and detection rates of HAHOBA on Oahu were modeled from nightly detector data. Multi-season dynamic occupancy models, which account for site-level extinction (the probability an occupied site will be unoccupied the next season) and local colonization (the probability an unoccupied site will be occupied the next season), were implemented to model trends in occupancy rates over time. Site-level covariates representing human population density, elevation, the percentage of trees, forest height, and land cover type in each grid cell were examined as predictors of occupancy.

Trends in occupancy were estimated in two ways: the mean annual proportional trend was calculated as the mean of the set of one-year proportional changes, and the net trend was calculated as the difference in occupancy in the first and last years divided by the first year occupancy estimate. The proportion of operating detectors with detections and 5-day moving averages of the daily proportions of detectors with detections were used to further examine the movement of bats over the course of the year.

The final dataset included data from 88 detectors, of which 86 of which were located in randomly selected cells and used in the occupancy analyses. The dataset spanned the period June 8, 2017, through the night of October 31, 2021 (the Study Period). At least one bat detection (i.e., bat call) was recorded during the Study Period at 84 (95%) of the 88 detectors monitored. The number of detector nights sampled by site during the Study Period ranged from 106 to 1,537 and 30,469

HAHOBA detections were recorded. The number of site-level detections ranged from zero to 6,083 during the Study Period. The mean number of site-level detections per detector night ranged from zero to 5.40 and the proportion of detector nights with detections ranged from zero to 0.45 during the Study Period. Detections were more widespread across Oahu during the post-lactation season relative to the other seasons.

The final model for the lactation season described occupancy as positively associated with the mean grid cell elevation and negatively associated with the indicator of any wet forest/grassland/shrub land cover in the cell. Estimated occupancy rates during the lactation season increased slightly during the Study Period, from 0.61 to 0.65. The final model for the post-lactation season contained no site-level covariates as predictors of site occupancy. Estimated occupancy rates during the post-lactation season increased slightly during the Study Period, from 0.75 to 0.81. The final model for the pre-pregnancy season contained a positive effect of mean grid cell elevation and a negative effect of the proportion of wet forest/grassland/shrub land cover. Estimated occupancy rates during the pre-pregnancy season increased during the Study Period, from 0.40 to 0.50. While occupancy estimates showed slight increases during the lactation, post-lactation, and pre-pregnancy seasons, the trend estimates during these seasons were not substantially different from zero. The final model for the pregnancy season contained a positive effect for elevation and negative effects for proportion of wet forest/grassland/shrub land cover and human population density within each grid cell. Estimated occupancy rates during the pregnancy season increased during the Study Period, from 0.31 to 0.46 and the trend estimates were substantially different from zero.

Occupancy rates varied by season, with the highest occupancy estimates observed in the lactation and post-lactation seasons and the lowest occupancy rates observed during the pre-pregnancy and pregnancy seasons. Bat occurrence (as indicated by the proportion of detectors with detections) expanded spatially over the pregnancy and lactation seasons, peaked near the beginning of the post-lactation season, and then contracted through the remainder of the post-lactation season to its most spatially restricted period during the pre-pregnancy. Occupancy rates exhibited slight but significant increasing trends in both mean and net proportional trends during the pregnancy season. Occupancy estimates during the other seasons had slight upward trajectories over the Study Period, but trends were not significant. Given the consistency in results across seasons and years, the HAHOBA occupancy rate for Oahu appeared stable to slightly increasing over the Study Period.

No habitat covariates were identified as significant predictors of site occupancy during the post-lactation season when the HAHOBA population appeared most dispersed across Oahu and occupancy rates were highest. The broader distribution and increased occupancy rates during this period could be indicative of a broader distribution of adult bats across the island or the dispersal of young-of-the-year bats recently added to the population or versus. Effects of elevation were positive and of similar magnitude for the three seasons incorporating site-level covariates in the occupancy model (lactation, pre-pregnancy, and pregnancy). The proportion of wet forest/grassland/shrub land cover was negatively associated with occupancy during these three seasons, with the negative effect increasingly pronounced in the pre-pregnancy and pregnancy

seasons. Mean monthly Oahu precipitation measured at weather stations between 1920 and 2012 ranged from 5.4 to 6.7 in (13.7 to 17.0 cm) per month from November through April, and from 3.1 to 4.6 in (7.9 to 11.7 cm) per month from May through October, defining distinct wet (November through April) and dry (May through October) periods on Oahu. Predicted HAHOBA occupancy across Oahu suggests that the drier mid-elevations are more consistently occupied throughout the year, while the leeward and more arid areas of the island are preferred during the rainy period, occurring principally during the pre-pregnancy season. Therefore, the HAHOBA distribution is most contracted during the wet period, when dry or mesic habitats appear to be preferred over wet habitats.

A power analysis was conducted to assess the sample size of detectors needed to detect 10% or 15% annual trends in lactation-season occupancy rates over a 10-year period. This prospective power analysis indicates that changes in occupancy over a 10-year period could be detected with reasonable power with a sample of 20–30 detectors. If a monitoring program were to be implemented over a longer term, we would suggest that the smaller samples would provide the best basis for inference if spatial balance and the probabilistic selection process used in this study were maintained so that the sampled population matches the target population as closely as possible. A fifth year of field data are being collected for a subsample of 40 of the 88 detectors reported on herein, which will be used to complete an updated analysis of trends in occupancy over a 5-year period.

STUDY PARTICIPANTS

Joel Thompson	Project Manager / Senior Biologist
Leigh Ann Starcevich	Senior Statistician
Erica Adamczyk	Field Biologist / Acoustic Analyst
David Young	Senior Reviewer
Mysti Martin	GIS Technician
Jeanette Haddock	Technical Editor
Kristina Hammond-Rendon	Bat Biologist / Acoustic Reviewer

ACKNOWLEDGEMENTS

REPORT REFERENCE

Thompson, J. and L. A. Starcevich. 2022. Oahu Hawaiian Hoary Bat. Occupancy and Distribution Study. Final Report. Prepared for Hawaii Endangered Species Research Committee. Prepared by Western EcoSystems Technology, Inc. Corvallis, Oregon. July 18, 2022

TABLE OF CONTENTS

LIST OF TABLES

LIST OF FIGURES

LIST OF APPENDICES

INTRODUCTION

In response to a request for proposals issued in 2016 by Hawaii's Endangered Species Recovery Committee (ESRC), Western EcoSystems Technology, Inc. (WEST) developed a 5-year study proposal to investigate the distribution and seasonal occupancy of Hawaiian hoary bat (HAHOBA; *Lasiurus cinereus semotus*) on the island of Oahu. The proposal was discussed during two meetings with the ESRC Bat subcommittee in January and February 2017, leading to a finalized study plan that focused on HAHOBA distribution and occupancy across the island of Oahu, in its entirety. The initial objectives of the study were to 1) provide information on bat occupancy, distribution, and detection probabilities for the island of Oahu, 2) examine seasonal changes in distribution by estimating seasonal changes in occupancy, and 3) collect data that could be used to assess HAHOBA habitat use relationships. The initial objectives were maintained throughout the study, with no substantial deviations to study design or data collection occurring over the four years of field studies.

Field data collection spanned a roughly 4-year period, beginning in late spring 2017 and concluding in early fall 2021. This final report is based on an updated analysis of the cumulative dataset spanning June 2017 to October 2021 (the Study Period). In this report, we describe the sampling design and methods used to collect and analyze the data and summarize the results and occupancy analysis through the fourth year of field studies. The report concludes with recommendations for concluding the study and future analysis, as well as thoughts on ways to continue the study in a meaningful, refined, and cost-effective manner.

This report represents the final analysis of data collected under the contractual obligations resulting from the 2016 ESRC request for proposals. As such, the data and analysis results presented herein supersede those presented in prior interim reports (e.g., Starcevich et al. 2019, 2020; Thompson and Starcevich 2021) and should be considered final as they relate to the full study conducted under obligation to the ESRC. However, an extension of the study was funded by several entities in early 2022 to collect additional data from a subset of sample locations, which will be incorporated into an updated analysis and report focused on annual trends in bat occupancy over a 5-year period.

METHODS

Sampling Design

The study design was developed to allow for island-wide inference. A sampling frame of 787 grid cells was developed in a geographic information system by overlaying a grid of 0.8-square mile (2.3-square kilometer) cells across the island of Oahu. To allow for island-wide inference, no areas on Oahu were omitted from the sampling frame except for small nearshore islands. From the grid of 787 cells, an equiprobable generalized random tessellation stratified sample (Stevens and Olsen 2003, 2004) of 100 grid cells was selected for the placement of acoustic bat detectors (Figure 1). An oversample of 150 grid cells was selected to provide an extra set of spatially

balanced sites to use if cells within the main sample could not be surveyed for some reason (e.g., inaccessibility due to safety issues, landowner denial of access).

Field Data Collection

Wildlife Acoustics Song Meter SM4Bat (SM4) full spectrum bat detectors fitted with model SMM-U1 (U1) ultrasonic microphones (Wildlife Acoustics, Inc., Concord, Massachusetts) were initially deployed for all data collection conducted by WEST. However, the U1 microphones began to malfunction in significant numbers in spring 2019. Based on the recommendations of the manufacturer, the U1 microphones were replaced with Wildlife Acoustics' newer SMM-U2 (U2) ultrasonic microphones. New U2 microphones were deployed throughout the summer and fall of 2019. The microphone type was recorded for each detector so that microphone effects could be examined as a covariate in detection probability models. Data collected by cooperating entities (e.g., Kuhuku Wind Project) and included in our analyses was collected using older Wildlife Acoustics full spectrum bat detectors (e.g., SM3Bat) outfitted with U1 microphones.

The SM4 detectors are small, measuring roughly eight inches (in) tall by five in wide by three in deep (20 centimeters [cm] tall by 13 cm wide by eight cm deep) and are fully self-contained (Figure 2). Some of the detectors located in easily accessible areas with relatively high risk of theft or vandalism were operated on internal batteries to minimize their detectability and potential vandalism or theft, while most detectors utilized a small external battery and accompanying solar panel as a power source (Figure 2).

Detectors were attached to existing structures (e.g., fence posts, light poles) or newly installed t-posts, via attachment of a 10-foot (ft; 3-meter [m]) length of 0.75 in (1.9 cm) diameter metal conduit used to extend the microphone approximately 10 ft above ground (Figure 2). In some cases, the 10-ft pole was supported by small guy wires. The detector, and external battery and solar panels (when used), were mounted low on the pole with the microphone mounted at the top of the pole (Figure 2). In some developed areas, units were contained in a small toolbox and placed on top of an appropriately sized outbuilding (approximately 10 ft above ground).
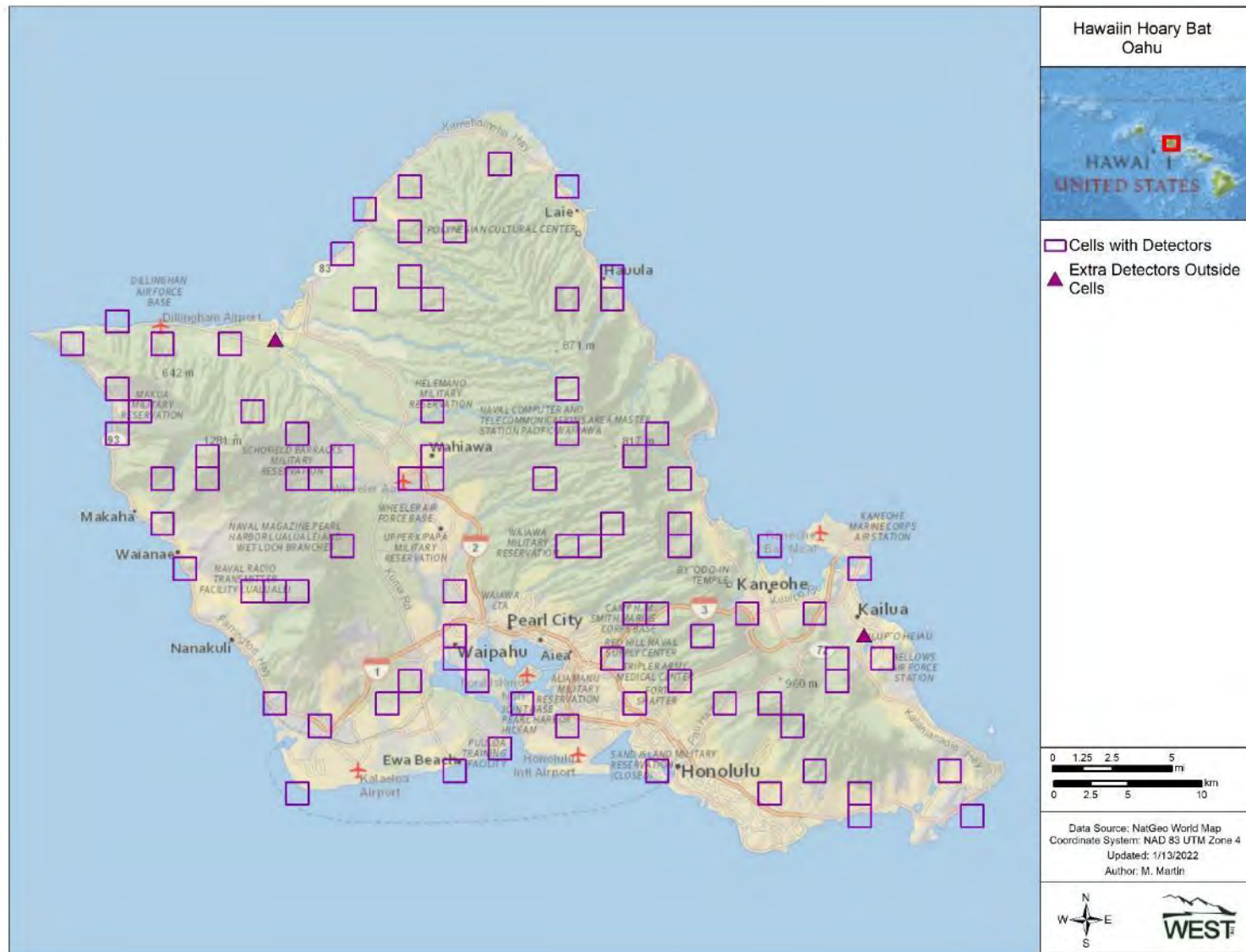
Figure 1.   Equiprobable generalized random tessellation stratified sample of 100 grid cells used for initial study design of the island-wide occupancy study of Hawaiian hoary bats on Oahu.
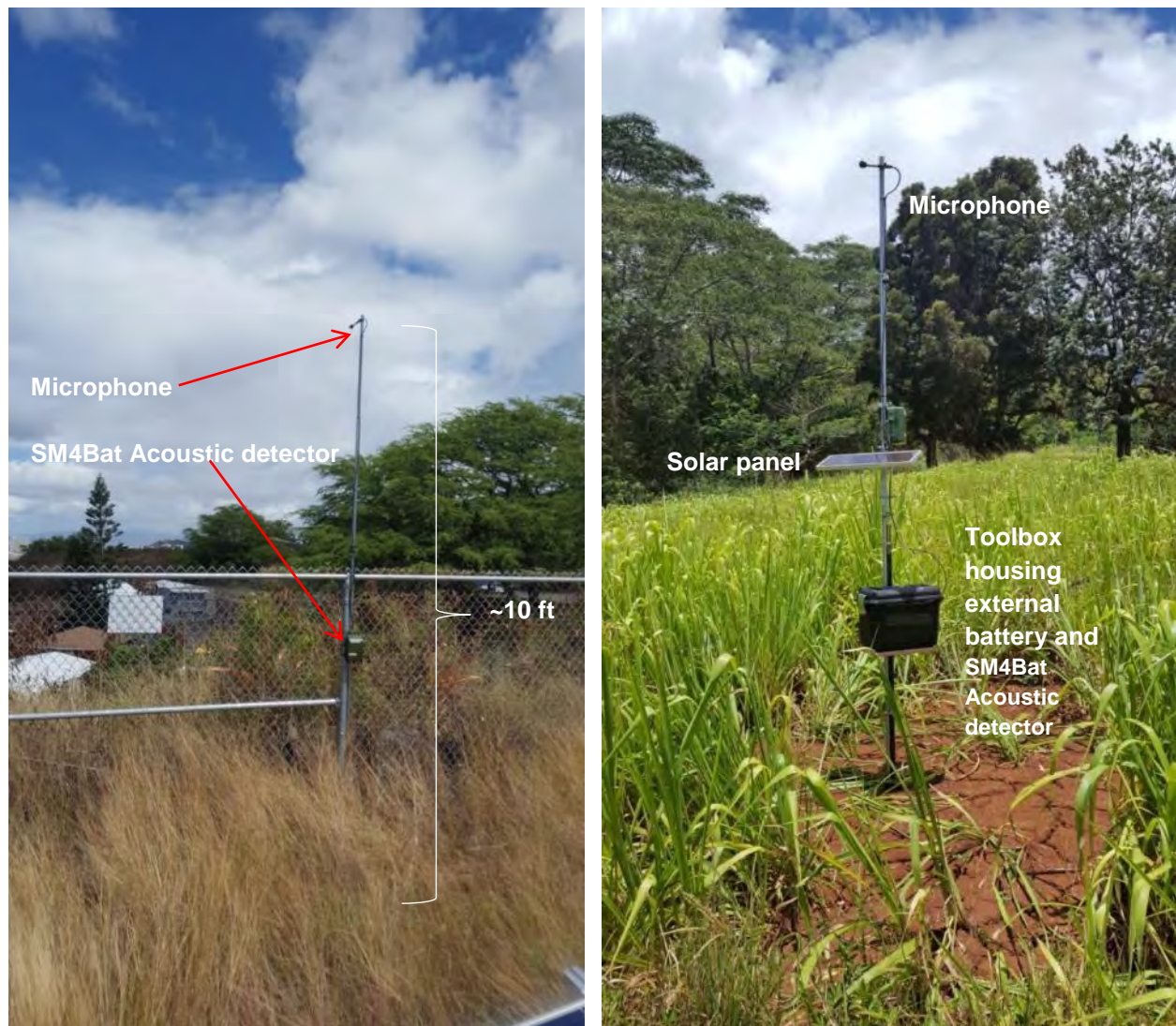
Figure 2.   Examples of commonly used set-ups of the Wildlife Acoustics SM4Bat detectors used in the Hawaiian hoary bat Occupancy and Distribution Study on Oahu.

Acoustic detectors remained in the field year round at the location of original placement. Detectors were programmed to operate nightly, from approximately one hour prior to sunset to approximately one hour after sunrise. Within the SM4 Detector Configurator, the following settings were selected: detector sample rate of 192 kilohertz (kHz); gain of 12 decibels (dB); minimum signal duration of 1.5 milliseconds; maximum signal duration off; minimum trigger frequency of 10 kHz; trigger level of 12 dB; and trigger window of three seconds. Detectors were visited regularly to swap data cards and inspect the units for proper function. Detectors were checked once seven to 14 days after initial deployment to ensure proper function and data collection, followed by less frequent checks. At sites with external power sources, detectors were checked every one to two months, while remote sites requiring helicopter access sometimes extended more than two months between checks. At sites where the detectors were powered by internal batteries, units were checked more frequently (e.g., every 10 to 14 days on average). However,

throughout much of 2020 and 2021, status checks were more sporadic due to the COVID-19 pandemic and resulting restrictions on access to parks, trails, helicopter use, and travel in general.

Call Analysis

To expedite call analysis, acoustic recordings were processed with the Kaleidoscope Pro 5 software package (Wildlife Acoustics 2019) to remove noise (i.e., non-bat) files and convert the full-spectrum call files to zero-cross files. For all files classified as containing a bat echolocation call, a bat biologist with training and experience in acoustic bat call analysis manually reviewed the zero-cross call files in program Analook (Titley Scientific) to ensure calls contained a minimum of two distinct pulses, and to confirm the recording was consistent with that of a HAHOBA. Manual review of all recorded bat calls by a bat biologist helped minimize the potential for false positives to be included in the final dataset. Social calls and feeding buzzes were noted during the manual review process for later assessment of behavioral activity at sites. A subset of noise files was also examined to ensure detectors were functioning properly when several consecutive nights without recordings occurred.

Occupancy Modeling

Acoustic detection data were examined using a dynamic occupancy analysis for correlated detections to obtain estimates of occupancy and detection rates. In the dynamic occupancy model for correlated detections, the detection probability is modeled conditional on both site occupancy and species availability. Occupancy and detection rates of HAHOBA on Oahu were modeled from nightly detector data, with the modeling approach informed by previous analyses (Starcevich et al. 2019, 2020; Thompson and Starcevich 2021). Multi-season dynamic occupancy models (MacKenzie et al. 2006), which account for site-level extinction (the probability an occupied site will be unoccupied the next season) and local colonization (the probability an unoccupied site will be occupied the next season), were implemented to model trends in occupancy rates. For comparability, reproductive seasons were defined consistent with those used by Gorresen et al. (2013, as adapted from Menard 2001) and used to define seasons within which closure was assumed. The reproductive seasons were defined as lactation (mid-June to August), post-lactation (September to mid-December), pre-pregnancy (mid-December to March), and pregnancy (April to mid-June). While these seasons were generally aligned with the reproductive cycle of HAHOBA, their purpose in this analysis was to define discrete seasons for analysis, not to suggest that the reproductive cycle of all HAHOBA are strictly aligned with these periods.

The multi-season dynamic occupancy model (MacKenzie et al. 2006) yields estimates of rates of occupancy (Ψ), detection (p), local extinction (ε), and local colonization (γ). The models we examined assumed closure within each reproductive season and modeled the local colonization and extinction rates as equal across all years. To relax the assumption of independent detections, the correlated detection model (Hines et al. 2014) was applied to account for the rate of local presence, the probability in which a species may temporarily emigrate from an occupied site and be unavailable for detection. Local presence was modeled conditionally on site occupancy and whether the species was locally present during the previous time period (θ_1) or not locally available at the previous time period (θ_0). The probability of detection (p) was modeled conditionally on local presence for the current and previous sampling occasion.

Previous analyses (Starcevich et al. 2019, 2020) applied the join count chi-square test (Wright et al. 2016) to evaluate the independence of nightly detection data within each reproductive season and year. The join count test compares the number of detections in consecutive time periods (temporal "joins") to an expected number based on the assumption of independence. Temporal correlation among detections violates the assumption of independent detections required for standard occupancy modeling. Failure to account for temporal correlation may result in variance underestimation, leading to narrow confidence intervals and inappropriately small p-values that indicate a significant effect when none exists. When temporal correlation is present, detection occasions may be separated in time to avoid temporal correlation (Wright et al. 2016). Previous analyses applied the join count test to data sets obtained from systematic random samples of detector nights taken by site at various intervals to determine the appropriate temporal spacing of detector nights. However, a small simulation of 25 iterations indicated that the correlated detection model adequately accounted for temporal correlation based on observed 95%-credible interval (CRI) coverage of 96% for Ψ and θ_0, 100% CRI coverage for θ_1 and p, and 92% CRI coverage for ε and γ. The slight under coverage for the dynamic occupancy parameters was considered negligible, and the full data set of consecutive nights was used for occupancy modeling.

All modeling was conducted in R (R Development Core Team 2021). The dynamic occupancy model for correlated detections (Hines et al. 2014) was applied in a Bayesian context with the *rjags* package (Plummer 2019). Modeling was conducted independently by reproductive season to estimate occupancy model parameters and the effects of site-level covariates for each season. We assumed uniform (0, 1) priors for all unknown probability parameters and vague Gaussian priors (Normal [0, 5]) for regression parameters. Three parallel Monte Carlo Markov chains were used, each sampling for 50,000 iterations after burn-in and adaptation phases of 5,000 iterations. Model diagnostics included convergence checks, trace plot review, and posterior predictive checking (Gelman et al. 2013). Site-level covariates (Table 1) representing human population density, elevation, the percentage of trees, forest height, and land cover type in each grid cell were examined as predictors of occupancy. Covariate effects were treated as correlated when more than one covariate was included in the model. Microphone type was used as a covariate for the detection probability model to account for any differences in detection rates potentially resulting from use of different microphone models (U1 or U2).

Model selection was conducted with the spike and slab approach (Mitchell and Beauchamp 1988). Spike and slab modeling is analogous to a LASSO method where all covariates are initially considered and unimportant covariates are assigned regression coefficients near zero. All site-level covariates were included in the model for initial occupancy, and posterior inclusion probabilities measured the importance of each covariate in the occupancy model. Covariates with posterior inclusion probabilities of 0.5 or more were included in the final occupancy model. The final model assumed correlated regression coefficients, but highly correlated covariates were excluded for model parsimony. A reduced model including only the important covariates was used for final inference so that interpretable credible intervals could be obtained.

Table 1.   Site-level covariates for occupancy modeling.

Site-level Covariate	Description
PopSqMi	Human population per square mile (mi) in each grid cell
PopSqMiClass	0 if population density <64.60 people per square mi, 1 otherwise
Elev	Mean site elevation in meters (m) in each grid cell
ElevClass	0 if elevation <144.62 m, 1 otherwise
PctTrees	Percent tree cover in grid cell
PctTreesClass	0 if percent tree cover <20.68, 1 otherwise
ForestHt_std	Standard deviation of forest height within grid cell
PropDry	Proportion of dry forest, grassland, or shrubland
PropDryClass	0 if PropDry=0, 1 if PropDry >0
PropMes	Proportion of mesic forest, grassland, or shrubland
PropMesClass	0 if PropMes=0, 1 if PropMes >0
PropWet	Proportion of wet forest, grassland, or shrubland
PropWetClass	0 if PropWet=0, 1 if PropWet >0

Trend was estimated in two ways: the mean annual proportional trend was calculated as the mean of the set of one-year proportional changes, and the net trend was calculated as the difference in occupancy in the first and last years divided by the first year occupancy estimate. The two-sided test for trend in occupancy was assessed by determining if the 95%-CRI for the mean proportional trend contained zero or the net proportional trend contained one, both of which indicate no substantial trend in occupancy. For example, a proportional trend (either the mean annual trend or the net trend over the monitoring period) of 0.08 implies an increase of 8% over the monitoring period, and a proportional trend of -0.08 is interpreted as an 8% decline in occupancy over the monitoring period.

The movement of bats over the course of the year was calculated as the proportion of operating detectors with detections and 5-day moving averages of the daily proportions of detectors with detections. Only nights with at least 20 operational detectors were used for occupancy modeling, which removed roughly the first two weeks of the study, and the data set was truncated to end August 31, 2021.

Power Analysis

The results of the occupancy analysis were used to inform an analysis of the power to detect an annual trend in occupancy over time. The power to detect annual linear trends of 10% and 15% in the occupancy rate over 10 years was assessed for sample sizes of 20, 40, 60, and 80 sites per year. A Monte Carlo simulation generated 500 populations with known occupancy, detection, and correlated detection parameters for the lactation season, and one of two trend levels was applied to each population. The correlated detection dynamic occupancy model (Hines et al. 2014) was applied to each simulated data set. The proportion of times that the 95%-CRI did not contain zero approximated the power of the two-sided test of a non-zero trend.

RESULTS

Detectors were deployed as access to sample sites was obtained, which resulted in a staggered start to data collection across sample sites. The first detectors were deployed in June 2017, with the initial deployment of detectors continuing through May 2018. Given the timing of initial detector deployments, the survey year is defined as beginning in the lactation season and extending through the end of the pregnancy season to reflect the timing of this study. For example, survey year 2017 spans the period June 15, 2017–June 14, 2018. While the initial goal was to deploy 100 detectors across Oahu, we were unable to achieve the goal of 100 detectors in Year 1 using the probabilistic sampling design. Land access was the most common reason for delay in getting units deployed within sequentially selected cells, with lack of suitable sample sites also causing some cells to be excluded from consideration. Land access issues were most often associated with cells mostly owned and/or managed by larger private landowners who would not grant access, or from whom we could not get a response to our request for access. In some cases, otherwise accessible cells lacked safely accessible sample sites or simply lacked a suitable location to mount or locate a detector. As a result of the various access issues, we extended our sample effort to include 19 of the oversample cells.

In total, WEST placed 86 acoustic detectors in the field, with 84 of the 86 located in randomly selected grid cells and two placed opportunistically at sites not within randomly selected cells (Figure 3). One other randomly selected grid cell was located in the Kuhuku Wind Project, which contained two detectors maintained and monitored by Kuhuku Wind Project personnel. One of the two Kuhuku detectors was randomly selected and the data included in our study dataset. In addition, data were incorporated into our final dataset from one detector monitored over a roughly 2-year period by the US Geological Survey (USGS) as a part of a larger study on Marine bases across Oahu (Pinzari et al. 2021), as this detector was located in one of the initial sample cells selected from the generalized random tessellation stratified sample. Due to vandalism and repeated theft, detectors at two locations (Ewa Beach Park and Malekahana State Park) were dropped from the sample relatively early (July 2018 and March 2019, respectively) in the Study Period, after at least two detectors and associated equipment were lost at each location. Of the two detectors not placed in randomly selected cells, one was located at a residence in Waialua and initially used as a test site, and the other was placed at Hamakua Ponds at the request of Department of Forestry and Wildlife staff. Data from these two detectors are reported, but the data were not used in the occupancy analyses. For the final analysis reported on herein, data were used from the 86 detectors located in randomly selected grid cells (84 deployed by WEST, Site-069 maintained by Kuhuku Wind, and Site-042 maintained by USGS).

Because detectors were placed in the field as access permissions were obtained, the temporal distribution of data varied among detectors. As such, seasonal data sets during the first year differ in the number of detectors that contributed data, as well as the number of nights contributed by individual detectors. While raw counts of bat calls are provided, due to the variability in sampling effort (i.e., the amount of time detectors were in the field) during the various years/seasons, the adjusted metrics of call counts/detector night and frequency of occurrence, not raw counts, were (and should be) used when making comparisons across seasons or years. The following sections

and appendices provided summary tables and figures presenting both raw counts and adjusted metrics in space and through time. A data visualization tool (*HAHOBA_Study.html*) is available as a supplement to this report, allowing for additional spatial and temporal sorting and display of the various datasets presented herein.

Detector Data

Total Detections

The final dataset spanned the period June 8, 2017, through the night of October 31, 2021 (the Study Period). Although the final date of data collection varied among detectors, 75% of detectors remained in the field through at least the end of July 2021. At least one bat detection (i.e., bat call) was recorded during the Study Period at 84 (95%) of the 88 (86 within randomly selected cells plus the two not in randomly selected cells) detectors monitored. The number of detector nights sampled by site during the Study Period ranged from 106 to 1,537 (Table 2), and 30,469 HAHOBA detections were recorded across all sites. The number of site-level detections ranged from zero to 6,083 during the Study Period (mean=346 detections, median=34 detections; Table 2).

Detections per Detector Night

The mean number of site-level detections per detector night ranged from zero to 5.40 among sites for all years combined during the Study Period (Table 2, Figure 4), with a maximum of 4.37 in Year 1, 5.19 in Year 2, 6.49 in Year 3, and 6.57 in Year 4 (Appendices A1–A4). Detections were more widespread across Oahu during the post-lactation season relative to the other seasons Appendices A5–A8).

Proportion of Detector Nights

The proportion of detector nights with detections ranged from zero to 0.45 (Table 2; Figure 5) across all seasons and sites for the Study Period, with annual variability from zero to 0.52 in Year 1, zero to 0.37 in Year 2, zero to 0.60 in Year 3, and zero to 0.46 in Year 4 (Appendices B1–B4). The proportion of detector nights with detections demonstrated seasonal patterns similar to those of mean detections per detector night, with a higher frequency of detections during the post-lactation season relative to the other seasons (Appendix B5–B8).

Feeding Buzzes and Social Calls

Feeding buzzes (n=1,485) were identified from call files recorded at 40 detectors, and social calls (n=129) from files recorded at 13 detectors (Figure 6). The presence of feeding buzzes and social calls is reported only for informational purposes. These two call types were treated the same as all other calls in the occupancy analyses.

Table 2. Total detections, total detector nights, mean detections per night, and proportion of nights with detections by site from June 8, 2017 to October 31, 2021.

Site ID	Site Name	Detections	Nights with Detections	Detector Nights[2]	Mean Detections Per Detector Night	Proportion of Detector Nights with Detections
Site-000	Goodale Tribe[1]	43	40	849	0.0506	0.0471
Site-002	TTHTT	39	35	1,157	0.0337	0.0303
Site-004	Army Nat Res	53	48	1,486	0.0357	0.0323
Site-006	Waihee Res	7	6	950	0.0074	0.0063
Site-008	Ewa Beach Park[3]	0	0	106	0	0
Site-009	Waianae HS	28	26	1,055	0.0265	0.0246
Site-011	Burn Camp	114	86	1,372	0.0831	0.0627
Site-013	KAW Gate	1,467	337	1,291	1.1363	0.2610
Site-016	Radar Hill Rd	32	28	980	0.0327	0.0286
Site-018	Dillingham Air	171	82	1,311	0.1304	0.0625
Site-020	Wahiawa botanical	25	23	1,438	0.0174	0.0160
Site-021	Lualualei 1	448	228	1,368	0.3275	0.1667
Site-022	Kahana Wedding	18	14	1,279	0.0141	0.0109
Site-023	Waimea Valley	975	387	1,344	0.7254	0.2879
Site-024	Ft Shafter	15	13	1,392	0.0108	0.0093
Site-025	Schofield	450	276	1,436	0.3134	0.1922
Site-026	Kawainiui	1	1	1,343	0.0007	0.0007
Site-029	KAW Rd	165	132	1,117	0.1477	0.1182
Site-030	Sacred Falls	3	3	1,182	0.0025	0.0025
Site-031	Plantation Village	7	7	1,351	0.0052	0.0052
Site-032	Nuuanu Watershed	1	1	1,316	0.0008	0.0008
Site-033	Camp Erdman	167	115	1,488	0.1122	0.0773
Site-034	Barbers Point	38	30	1,224	0.0310	0.0245
Site-035	Helemano	90	80	1,422	0.0633	0.0563
Site-036	Kroc Center	17	14	1,341	0.0127	0.0104
Site-038	Moanalua Trail	1	1	1,392	0.0007	0.0007
Site-039	Pupukea	4,237	389	1,310	3.2344	0.2969
Site-040	Hickham AFB	0	0	1,237	0	0
Site-041	Schofield 3	1,208	455	1,386	0.8716	0.3283
Site-042	042 USGS	1	1	676	0.0015	0.0015
Site-043	Manana Trail 1	6	6	1,350	0.0044	0.0044
Site-044	Royal Hawaiian Golf	7	6	1,297	0.0054	0.0046
Site-046	Poamoho	24	22	1,342	0.0179	0.0164
Site-048	Chaminade Univ.	38	29	1,524	0.0249	0.0190
Site-049	Lualualei NAVY	80	64	1,368	0.0585	0.0468
Site-050	HECO Kahe Point	6	4	905	0.0066	0.0044
Site-053	Kumaipo LZ	6,083	504	1,127	5.3975	0.4472
Site-054	Anchor Church	8	8	1,199	0.0067	0.0067
Site-055	Schofield Waikane	48	38	1,207	0.0398	0.0315
Site-057	McCarthy Field	304	220	1,483	0.2050	0.1483
Site-058	Kailua Heights	7	6	1,199	0.0058	0.0050
Site-059	Moanalua Red Hill	11	10	1,301	0.0085	0.0077
Site-060	Hawaii Loa Booster	23	23	1,316	0.0175	0.0175
Site-061	Mt Kaala	696	453	1,488	0.4677	0.3044
Site-064	Kamehameha Res	36	29	931	0.0387	0.0311
Site-065	Makua Valley	93	64	1,320	0.0705	0.0485
Site-066	Wheeler	93	84	1,430	0.0650	0.0587
Site-067	Honouliuli FR	77	55	1,015	0.0759	0.0542
Site-068	Waikane Valley	4	3	748	0.0053	0.0040

Table 2. Total detections, total detector nights, mean detections per night, and proportion of nights with detections by site from June 8, 2017 to October 31, 2021.

Site ID	Site Name	Detections	Nights with Detections	Detector Nights[2]	Mean Detections Per Detector Night	Proportion of Detector Nights with Detections
Site-069	MitchDetector	7	5	1,496	0.0047	0.0033
Site-070	Iroquois Pt	63	49	1,268	0.0497	0.0386
Site-071	Makaha Res	75	51	1,224	0.0613	0.0417
Site-072	Waihee Wells	0	0	1,207	0	0
Site-073	Kipapa North Fence	0	0	271	0	0
Site-074	Hawaii Loa	74	46	1,316	0.0562	0.0350
Site-075	Peerson	4,023	561	1,380	2.9152	0.4065
Site-076	Kaipapau FR	42	15	902	0.0466	0.0166
Site-077	Manana Trail 2	10	10	1,372	0.0073	0.0073
Site-078	Sand Island	7	7	1,315	0.0053	0.0053
Site-079	Makua Ridge	971	358	1,433	0.6776	0.2498
Site-081	KAW 2	160	113	1,215	0.1317	0.0930
Site-083	Lualualei 2	217	122	1,119	0.1939	0.1090
Site-084	Aiea Loop Ridge	8	8	1,201	0.0067	0.0067
Site-085	Kaw 1	119	103	1,331	0.0894	0.0774
Site-087	Schofield 1	207	161	1,394	0.1485	0.1155
Site-088	Kawainui Marsh 1	1	1	1,263	0.0008	0.0008
Site-089	Waiawa Snot	19	13	1,334	0.0142	0.0097
Site-090	Kau Crater Trail	1	1	1,341	0.0007	0.0007
Site-093	Pouhala Marsh	7	7	1,061	0.0066	0.0066
Site-094	Manoa Falls	8	6	1,485	0.0054	0.0040
Site-095	Kuaokala Game Area	2,819	165	1,309	2.1536	0.1261
Site-097	Malaekahana SP	152	14	509	0.2986	0.0275
Site-098	West Loch Golf	17	16	1,068	0.0159	0.0150
Site-100	Heeia State Park	9	8	1,537	0.0059	0.0052
Site-101	Pupukea Paumalu	805	329	1,132	0.7111	0.2906
Site-102	Pearl Harbor	22	19	1,262	0.0174	0.0151
Site-103	Schofield Forest	1,270	312	1,456	0.8723	0.2143
Site-105	Aiea Loop Trail 1	237	64	1,438	0.1648	0.0445
Site-106	Puu Pia Trail	2	2	1,179	0.0017	0.0017
Site-109	Central Oahu Park	18	16	1,140	0.0158	0.0140
Site-110	Halone Blowhole	40	27	1,261	0.0317	0.0214
Site-111	YMCA Waianae	46	36	679	0.0677	0.0530
Site-112	Barbers Point	1	1	1,102	0.0009	0.0009
Site-113	Hauula Dist. Park	10	7	1,124	0.0089	0.0062
Site-114	Waipio Soccer	3	3	1,168	0.0026	0.0026
Site-115	Waianae Valley	1,250	165	1,318	0.9484	0.1252
Site-119	Makua Cave	280	140	1,082	0.2588	0.1294
Site-999	Hamakua Pond[1]	4	4	979	0.0041	0.0041

[1.] Denotes subjectively selected grid cells.

[2.] Denotes nights that the detector was functional.

[3.] Denotes data from a single season only.
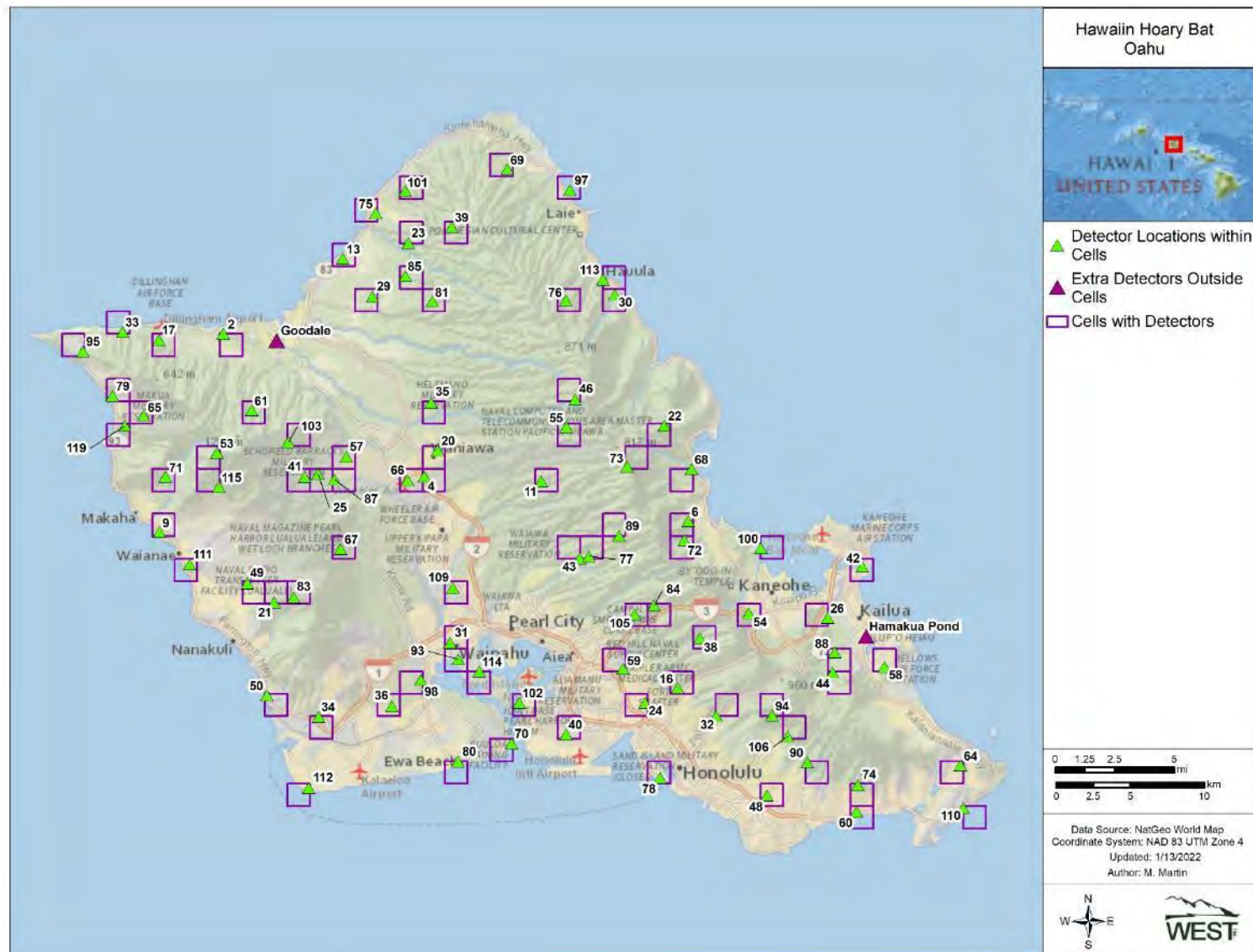
Figure 3. Distribution of acoustic bat detectors used in the island-wide occupancy study of Hawaiian hoary bats on Oahu. Site identification numbers provided for each sample location.
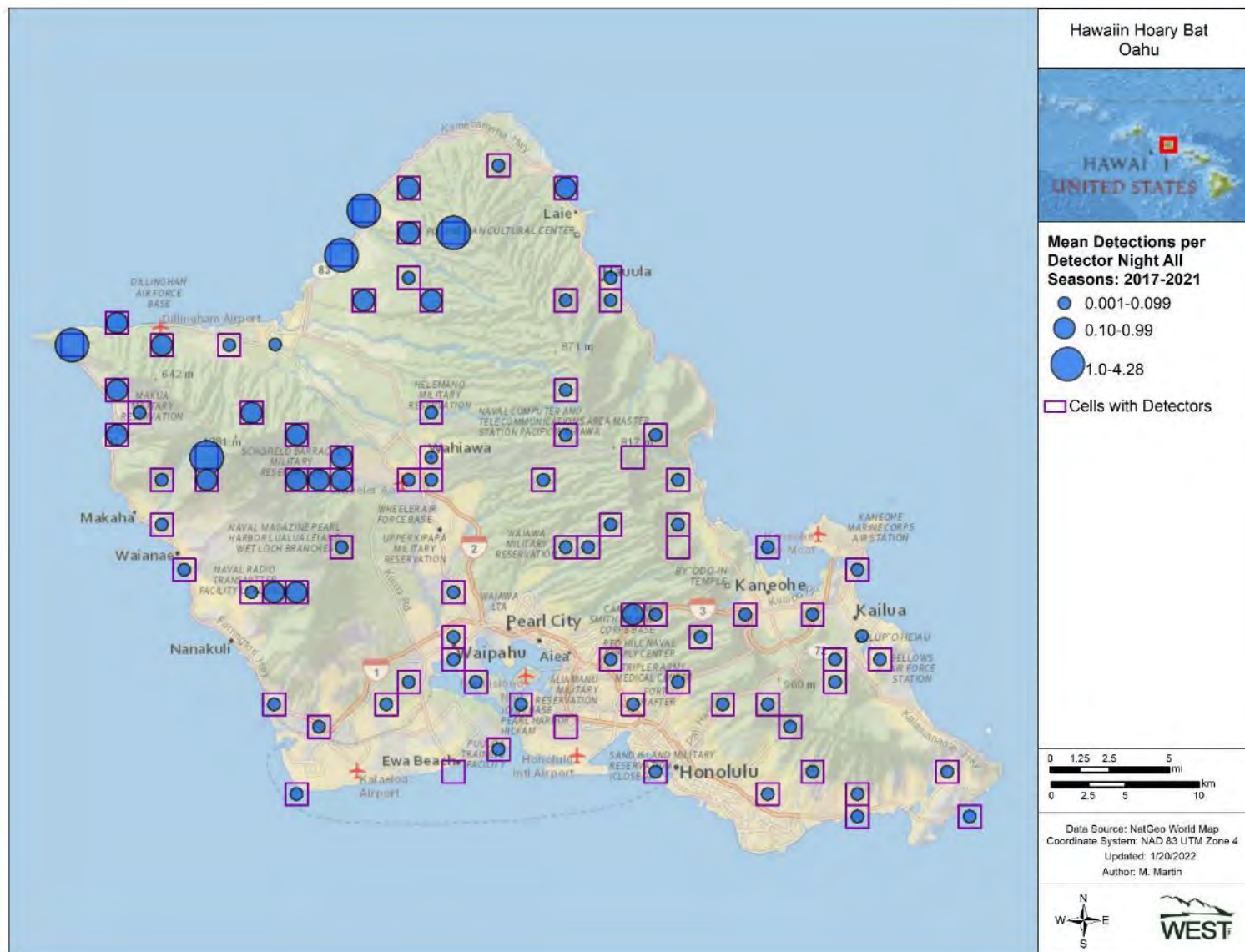
Figure 4.   Mean detections per night by site between June 8, 2017 and October 31, 2021.
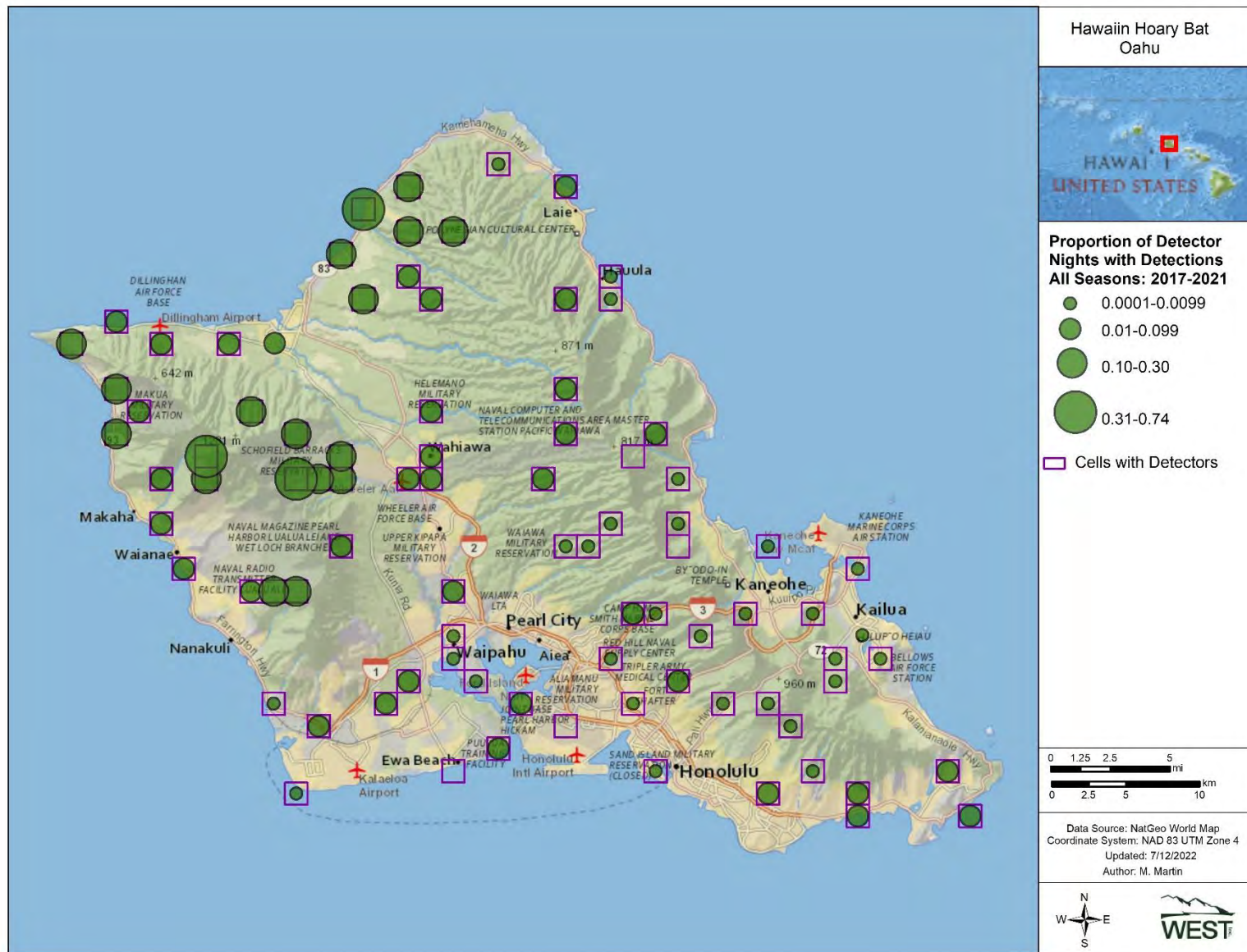
Figure 5.   Proportion of nights with detections by site between June 8, 2017 and October 31, 2021.
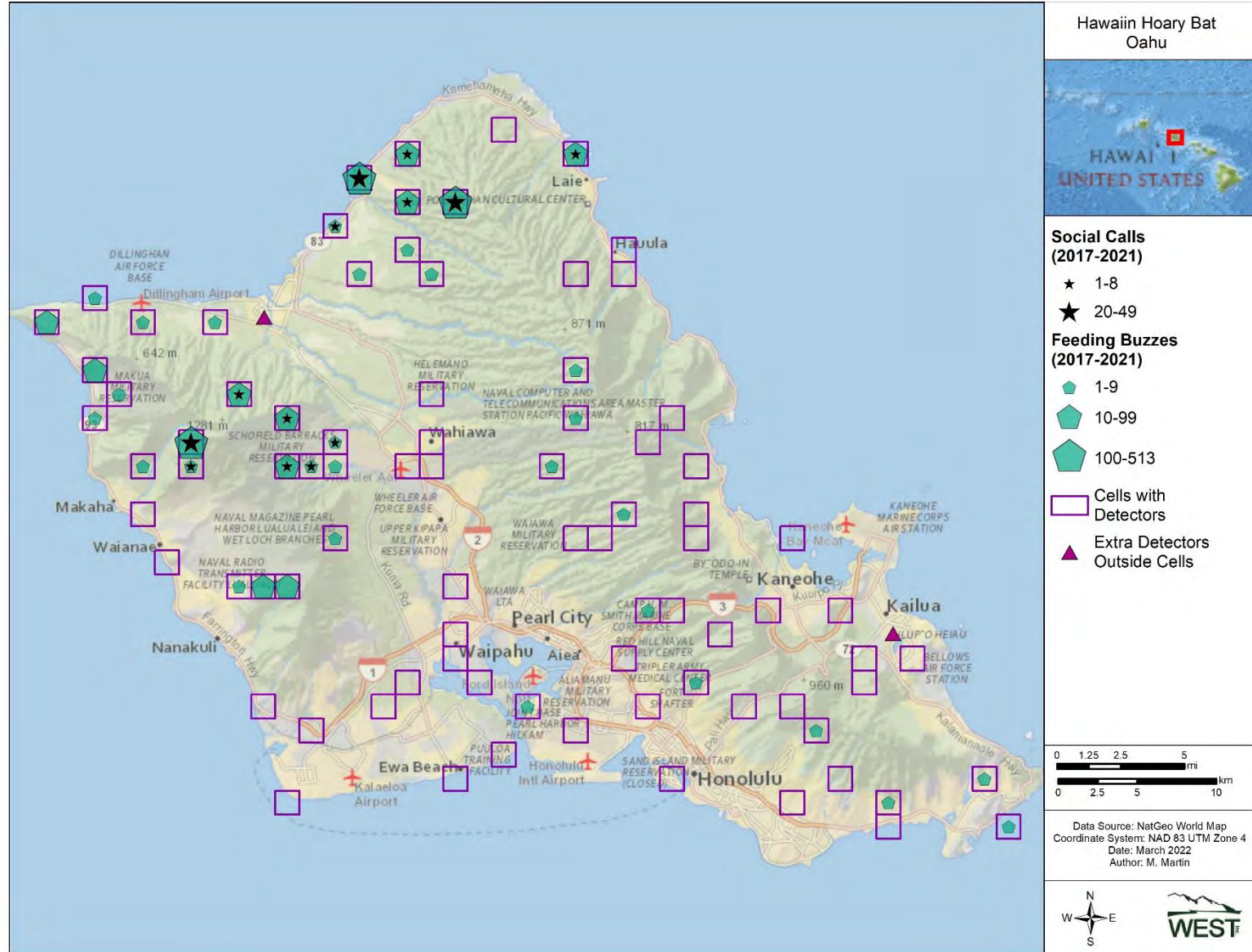
Figure 6. Distribution of feeding buzzes and social calls recorded between June 8, 2017 and October 31, 2021.

Occupancy Modeling

Site-level covariates (Table 3) used to model occupancy included human population per square mile (US Census Bureau 2019), mean elevation of the grid cell in meters (USGS 2017), the percentage of the grid cell covered in tree-dominated land cover classes (LANDFIRE 2017), and the standard deviation of tree height in each grid cell. Several site-level covariates were also discretized into a two-level category of low/high based on the median value and are indicated as covariates ending in "Class." To improve model convergence, human population density was scaled to density per thousand people, and elevation was scaled to hectometers (100 m [328 ft]). The distribution of each of the site-level covariates, with the exception of forest height standard deviation, was skewed right with a high proportion of values near zero (Table 3, Figures 7 and 8).

Table 3. **Summary statistics for site-level covariates for all grid cells in the sampling frame and the subset of grid cells in the sample.**

| Site-level Covariate	Sampling Frame			Sample		
	Mean	Median	Range	Mean	Median	Range
PopSqMi (number/mile^2)	1,390.5	64.6	0–33,319.9	1,114.3	188.4	0–13,759.0
Elev (meters)	188.9	141.4	0–896.7	187.2	144.6	0.1–643.1
PctTrees (%)	37.3	20.7	0–99.8	37.9	24.5	0–99.1
ForestHt_std	4.2	4.1	0–12.8	4.4	4.5	0.4–9.0
PropDry (%)	19.8	3.7	0–99.9	0.2	0	0–1.0
PropMes (%)	22.3	0	0–99.6	0.2	0	0–1.0
PropWet (%)	14.8	0	0–100	0.1	0	0–1.0

Figure 7. **Distribution of site-level covariates measuring grid cell human population density, mean elevation, percent tree cover, and the standard deviation in forest height.**

Figure 8. **Distribution of site-level covariates measuring grid cell proportions of forest, grassland, or shrubland classified as dry, mesic, or wet.**
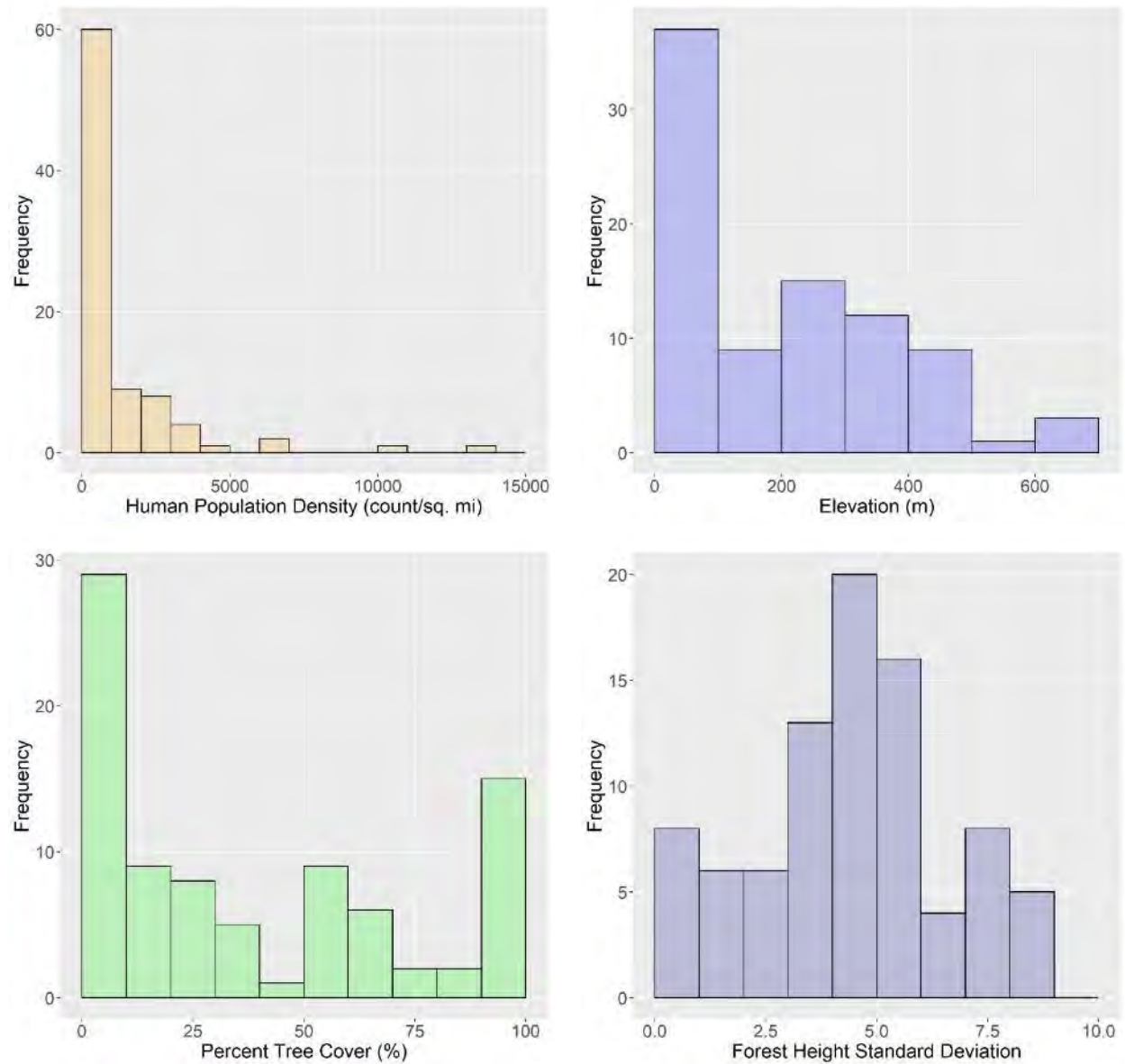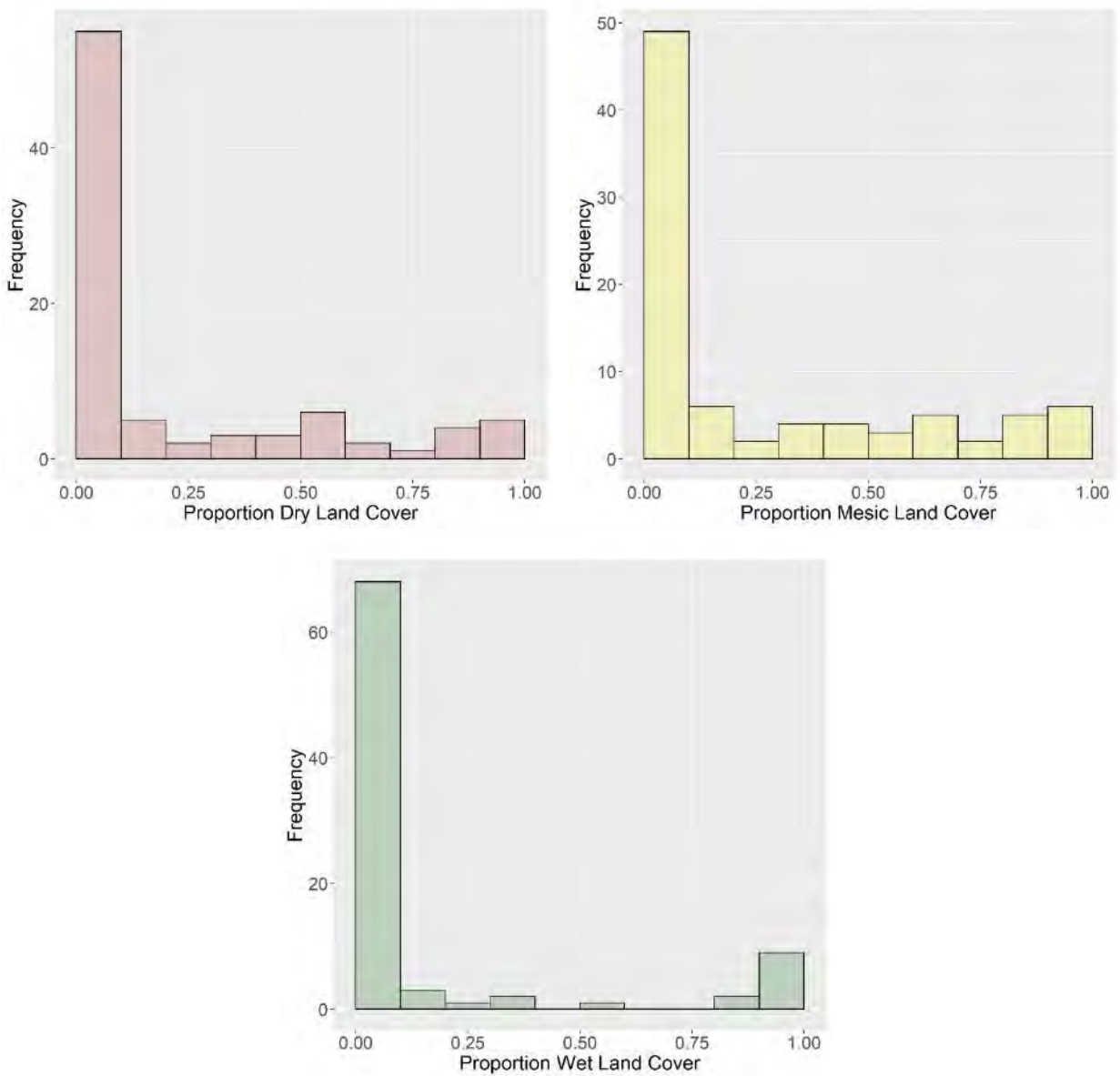
Model parameters are defined in Table 4. Intercept-only models were used to model local extinction and local colonization. The final models for each reproductive season are provided in Tables 5–8.

Table 4. **Occupancy model parameters for the multi-season dynamic occupancy model for correlated detections (Hines et al. 2014).**

Parameter	Description
psi	Occupancy rate.
theta0	Probability the species is available at a survey occasion given the site is occupied and the species **was not** available at the previous survey occasion.
theta1	Probability the species is available at a survey occasion given the site is occupied and the species **was** available at the previous survey occasion.
gam	Probability a site not occupied during a given season is colonized during the next season.
eps	Probability a site occupied during a given season is not occupied during the next season.
p	Probability a species is detected given the site is occupied and the species is currently available.

The final model for the lactation season (Table 5) described occupancy as positively associated with the mean grid cell elevation and negatively associated with the indicator of any wet forest/grassland/shrub land cover in the cell. Estimated occupancy rates during the lactation season (Table 9, Figure 9) increased slightly during the Study Period, from 0.61 (95%-CRI: 0.50, 0.74) to 0.65 (95%-CRI: 0.55, 0.74). However, the trend estimates were not substantially different from zero, as evidenced by the 95%-CRI on the occupancy estimates (Table 5), the mean proportional trend (0.01, 95%-CRI: -0.05, 0.08) for which the CRI overlapped zero, and the net proportional trend (1.07, 95%-CRI: 0.82, 1.36) for which the CRI overlapped one. The estimated detection probability (Table 10, Figure 10) for the U1 microphone (0.44, 95%-CRI: 0.40, 0.48) was slightly higher than for the U2 microphone (0.38, 95%-CRI: 0.35, 0.42) during the lactation season (difference in detection rates: 0.05, 95%-CRI: 0.02, 0.09).

The final model for the post-lactation season (Table 6) contained no site-level covariates as predictors of site occupancy. Estimated occupancy rates during the post-lactation season increased slightly during the Study Period (Table 9, Figure 9), from 0.75 (95%-CRI: 0.63, 0.87) to 0.81 (95%-CRI: 0.74, 0.88). However, the trend estimates were not substantially different from zero, as evidenced by the 95%-CRI on the occupancy estimates (Table 6), mean proportional trend (0.02, 95%-CRI: -0.02, 0.08), and net proportional trend (1.09, 95%-CRI: 0.91, 1.32). Detection probabilities (Table 10, Figure 10) were modeled by microphone type (Table 6, Figure 10), with slightly higher detection for the U2 microphone (0.34, 95%-CRI: 0.32, 0.36) than the U1 microphone (0.20, 95%-CRI: 0.18, 0.22). This difference was substantially different from zero (mean difference: -0.14, 95%-CRI: -0.16, -0.12).

The final model for the pre-pregnancy season (Table 7) contained a positive effect of mean grid cell elevation and a negative effect of the proportion of wet forest/grassland/shrub land cover. Estimated occupancy rates during the pre-pregnancy season (Table 9, Figure 9) increased during

the Study Period, from 0.40 (95%-CRI: 0.32, 0.49) to 0.50 (95%-CRI: 0.39, 0.61). However, the trend estimates were not substantially different from zero, as evidenced by the 95%-CRI on the occupancy estimates (Table 7), the mean proportional trend estimate (0.08, 95%-CRI: -0.02, 0.19) and net proportional trend (1.26, 95%-CRI: 0.93, 1.66). The detection rate (Table 7, Figure 10) was estimated for the U1 microphone as 0.20 (95%-CRI: 0.18, 0.23) and for the U2 microphone as 0.28 (95%-CRI: 0.25, 0.31). The detection probability (Table 10, Figure 10) for the U1 microphone was lower than for the U2 microphone (mean difference: -0.07, 95%-CRI: -0.11, -0.04).

The final model for the pregnancy season (Table 8) contained a positive effect for elevation and negative effects for proportion of wet forest/grassland/shrub land cover and human population density within each grid cell. Estimated occupancy rates during the pregnancy season (Table 9, Figure 9) increased during the Study Period, from 0.31 (95%-CRI: 0.24, 0.38) to 0.46 (95%-CRI: 0.36, 0.57). The trend estimates were substantially different from zero, as evidenced by the 95%-CRI on the occupancy estimates (Table 8), the mean proportional trend (0.15, 95%-CRI: 0.04, 0.28), and the net proportional trend (1.53, 95%-CRI: 1.12, 2.04). The detection probability (Table 10, Figure 10) for the U1 microphone (0.32, 95%-CRI: 0.29, 0.36) was lower than for the U2 microphone (0.42, 95%-CRI: 0.38, 0.46) with a mean difference of -0.10 (95%-CRI: -0.14, -0.05).

Table 5. Correlated detection occupancy model estimates, standard error (SE), and credible intervals (CRI) for the Lactation season.

Parameter	Mean	SE	95%-CRI Lower Bound	95%-CRI Upper Bound
p[1]: U1 mic	0.44	0.02	0.40	0.48
p[2]: U2 mic	0.38	0.02	0.35	0.42
psivec[1]	0.61	0.06	0.50	0.74
psivec[2]	0.63	0.04	0.56	0.70
psivec[3]	0.64	0.04	0.56	0.71
psivec[4]	0.64	0.04	0.56	0.73
psivec[5]	0.65	0.05	0.55	0.74
beta0	2.37	0.94	0.92	4.54
beta: Elev	2.64	0.95	1.19	4.87
beta: PropWetClass	-4.14	1.61	-7.81	-1.55
gam	0.31	0.05	0.22	0.40
eps	0.17	0.03	0.11	0.23
meanPropTrend	0.01	0.03	-0.05	0.08
netPropTrend	1.07	0.14	0.82	1.36
theta0	0.06	0	0.05	0.07
theta1	0.90	0.01	0.88	0.92
pi	0.38	0.04	0.30	0.47

Table 6. Correlated detection occupancy model estimates, standard error (SE), and credible intervals (CRI) for the Post-Lactation season.

Parameter	Mean	SE	95%-CRI Lower Bound	95%-CRI Upper Bound
p[1]: U1 mic	0.20	0.01	0.18	0.22
p[2]: U2 mic	0.34	0.01	0.32	0.36
psivec[1]	0.75	0.06	0.63	0.87
psivec[2]	0.80	0.03	0.73	0.85
psivec[3]	0.81	0.03	0.74	0.87
psivec[4]	0.81	0.03	0.74	0.88
psivec[5]	0.81	0.03	0.74	0.88
beta0	1.15	0.34	0.52	1.86
gam	0.56	0.07	0.41	0.69
eps	0.13	0.03	0.08	0.18
meanPropTrend	0.02	0.03	-0.02	0.08
netPropTrend	1.09	0.11	0.91	1.32
theta0	0.04	0	0.04	0.05
theta1	0.95	0.01	0.94	0.96
pi	0.41	0.04	0.33	0.50

Table 7. Correlated detection occupancy model estimates, standard error (SE), and credible intervals (CRI) for the Pre-Pregnancy season.

Parameter	Mean	SE	95%-CRI Lower Bound	95%-CRI Upper Bound
p[1]: U1 mic	0.20	0.01	0.18	0.23
p[2]: U2 mic	0.28	0.02	0.25	0.31
psivec[1]	0.40	0.04	0.32	0.49
psivec[2]	0.45	0.04	0.38	0.53
psivec[3]	0.48	0.05	0.39	0.57
psivec[4]	0.50	0.06	0.39	0.61
beta0	0.57	0.44	-0.21	1.53
beta[1]: Elev	2.14	0.54	1.19	3.33
beta[2]: PropWet	-7.16	2.05	-11.73	-3.73
gam	0.20	0.04	0.13	0.28
eps	0.18	0.06	0.08	0.30
meanPropTrend	0.08	0.05	-0.02	0.19
netPropTrend	1.26	0.19	0.93	1.66
theta0	0.03	0	0.03	0.04
theta1	0.93	0.01	0.91	0.94
pi	0.28	0.05	0.18	0.39

Table 8. Correlated detection occupancy model estimates, standard error (SE), and credible intervals (CRI) for the Pregnancy season.

Parameter	Mean	SE	95%-CRI Lower Bound	95%-CRI Upper Bound
p[1]: U1 mic	0.32	0.02	0.29	0.36
p[2]: U2 mic	0.42	0.02	0.38	0.46
psivec[1]	0.31	0.04	0.24	0.38
psivec[2]	0.38	0.03	0.31	0.45
psivec[3]	0.43	0.04	0.34	0.52
psivec[4]	0.46	0.05	0.36	0.57
beta0	1.10	0.70	-0.17	2.56
beta[1]: Elev	2.47	0.68	1.29	3.93
beta[2]: PropWet	-18.22	6.40	-32.44	-7.92
beta[3]: PopSqMiClass	-1.94	0.87	-3.77	-0.35
gam	0.16	0.03	0.10	0.23
eps	0.14	0.05	0.06	0.24
meanPropTrend	0.15	0.06	0.04	0.28
netPropTrend	1.53	0.23	1.12	2.04
theta0	0.05	0.01	0.04	0.06
theta1	0.90	0.01	0.88	0.92
pi	0.37	0.06	0.26	0.48

Table 9. Estimated occupancy rates and credible intervals (CRI) by season and year.

Season	Year	Estimated Occupancy	95%-CRI Lower Bound	95%-CRI Upper Bound
Lactation	2017	0.61	0.50	0.74
	2018	0.63	0.56	0.70
	2019	0.64	0.56	0.71
	2020	0.64	0.56	0.73
	2021	0.65	0.55	0.74
Post-Lactation	2017	0.75	0.63	0.87
	2018	0.80	0.73	0.85
	2019	0.81	0.74	0.87
	2020	0.81	0.74	0.88
	2021	0.81	0.74	0.88
Pre-Pregnancy	2017	0.40	0.32	0.49
	2018	0.45	0.38	0.53
	2019	0.48	0.39	0.57
	2020	0.50	0.39	0.61
Pregnancy	2017	0.31	0.24	0.38
	2018	0.38	0.31	0.45
	2019	0.43	0.34	0.52
	2020	0.46	0.36	0.57

Table 10.   Estimated detection rates and credible intervals (CRI) by season and microphone type.

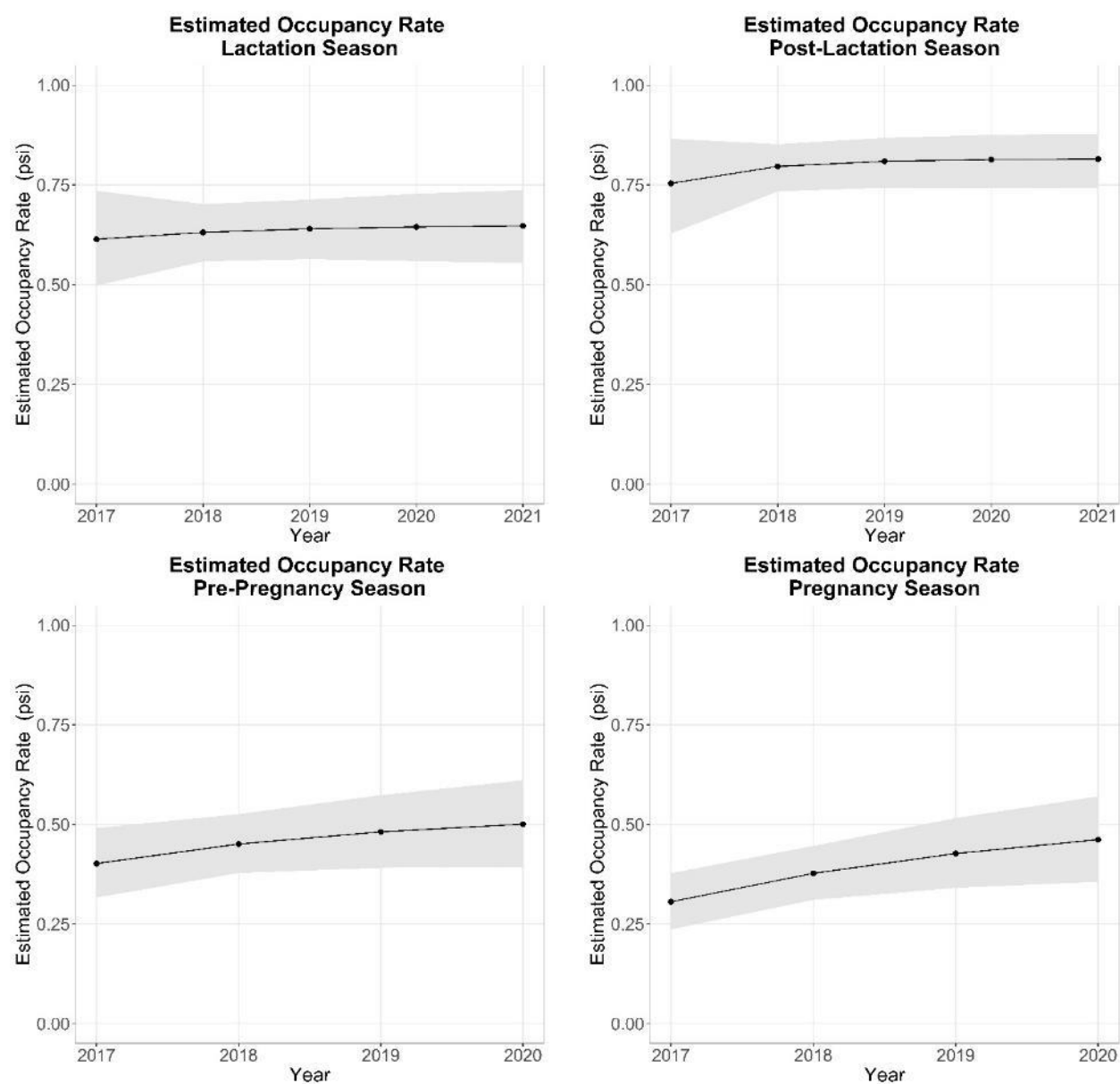| Season	Mic Type	Estimated Occupancy	95%-CRI Lower Bound	95%-CRI Upper Bound
Lactation	U1	0.44	0.40	0.48
	U2	0.38	0.35	0.42
Post-Lactation	U1	0.20	0.18	0.22
	U2	0.34	0.32	0.36
Pre-Pregnancy	U1	0.32	0.29	0.36
	U2	0.42	0.38	0.46
Pregnancy	U1	0.20	0.18	0.23
	U2	0.28	0.25	0.31

Figure 9.   Occupancy estimates and 95% credible intervals by reproductive season and year.
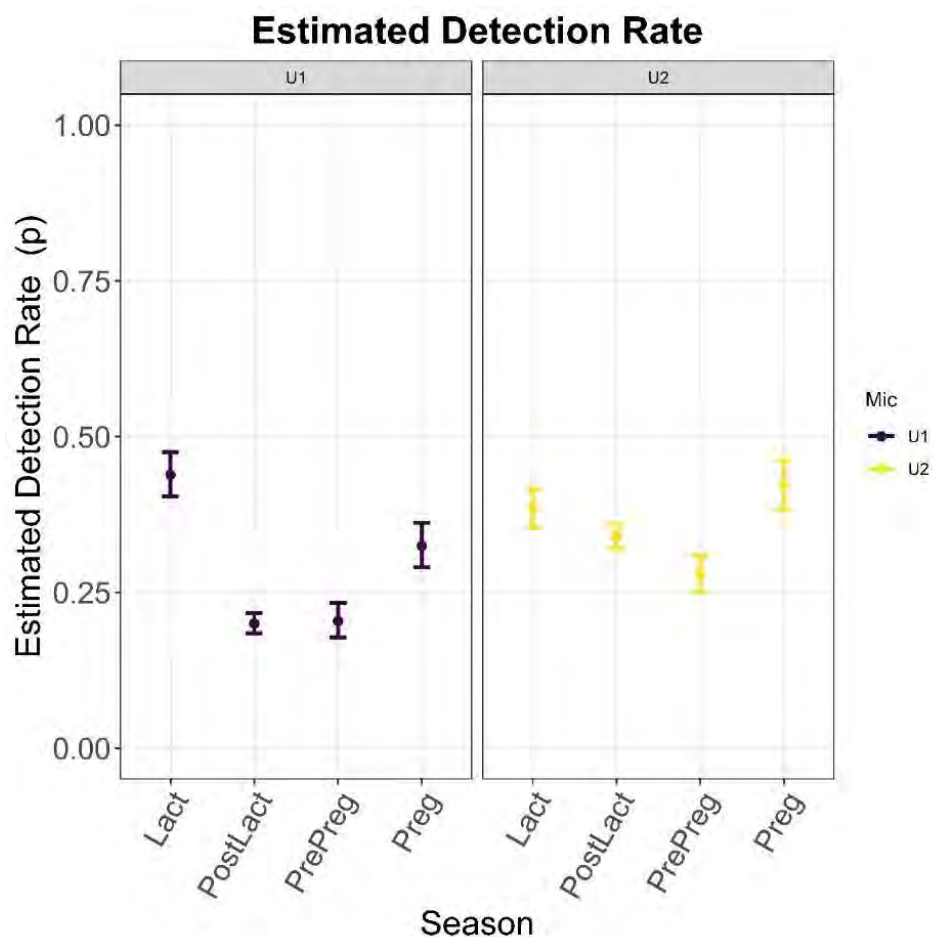
Figure 10. Detection probability estimates and 95% confidence bands by reproductive season and microphone type.

Heat maps of occupancy were developed from the final models for each season (Figure 11). With the exception of the post-lactation season, for which no site-level covariates were identified as important predictors, occupancy was modeled as a function of mean grid cell elevation and the proportion of the wet forest/grassland/shrub land cover type. Occupancy during the pregnancy season was additionally modeled as a function of human population density. Heat maps indicate areas with a high probability of being consistently occupied in a given season, and a comparison of maps provides indication of areas with a high probability of occupancy throughout the year.
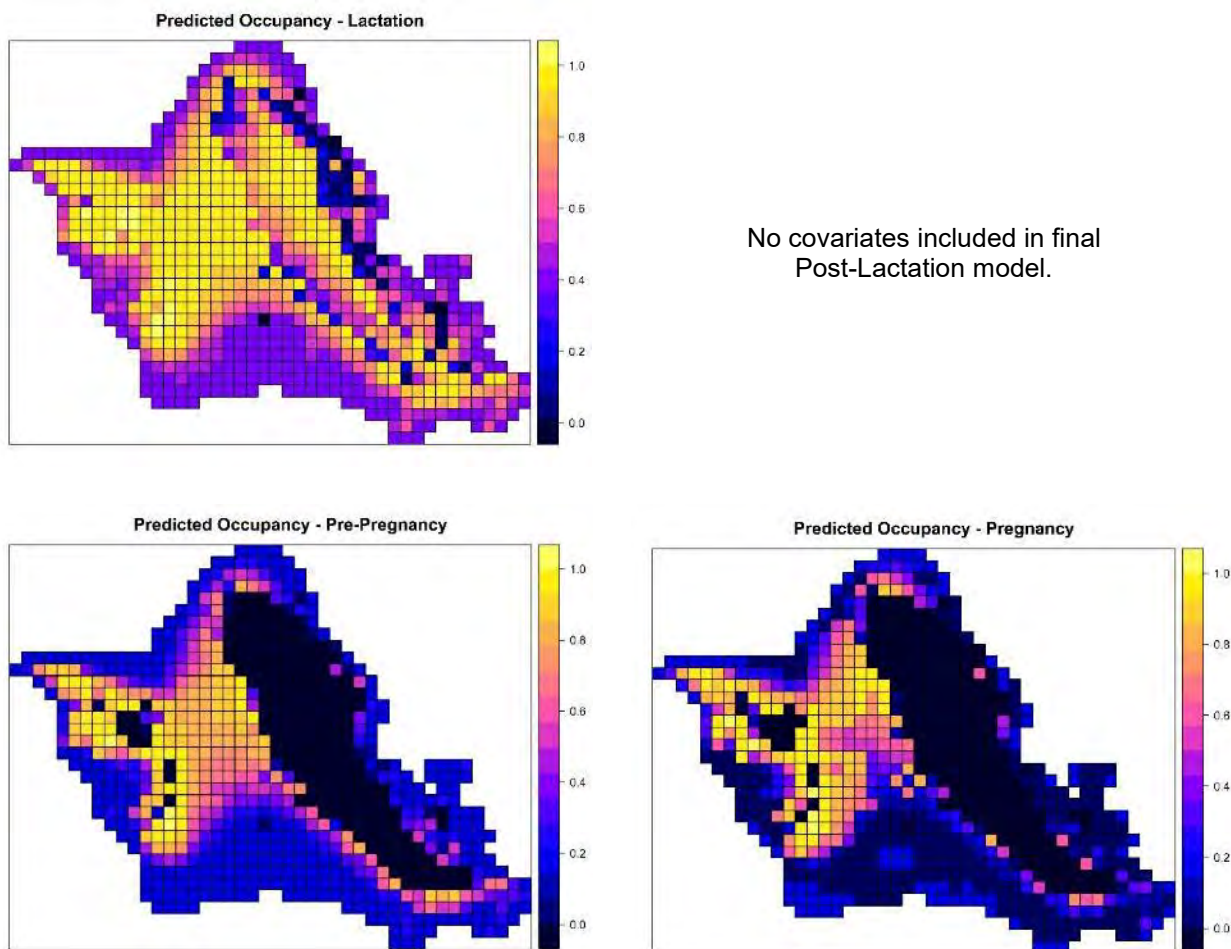
No covariates included in final
Post-Lactation model.

Figure 11. Predicted occupancy by season.

The relationship between elevation and the proportion of wet forest/grassland/shrub land cover was examined for the range of possible values by season (Figure 12). Occupancy rates during the lactation season were modeled as a function of the indicator of *any* wet forest/grassland/shrub in a grid cell, therefore estimates of occupancy differ for proportions of zero cover versus any non-zero cover. Preferred habitat in the lactation season is represented in green and includes areas above 100 m with no wet forest/grassland/shrub cover and areas above 300 m (984 ft) elevation with any wet forest/grassland/shrub cover. During the pre-pregnancy season, wetter areas (e.g., greater than 60% wet forest/grassland/shrub) are predicted to be occupied only at higher elevations, whereas during the pregnancy season, wetter areas are not predicted to be occupied, regardless of elevation. The post-lactation occupancy model did not include habitat covariates so we infer no preference by HAHOBA of specific elevations or land cover types during this reproductive season.

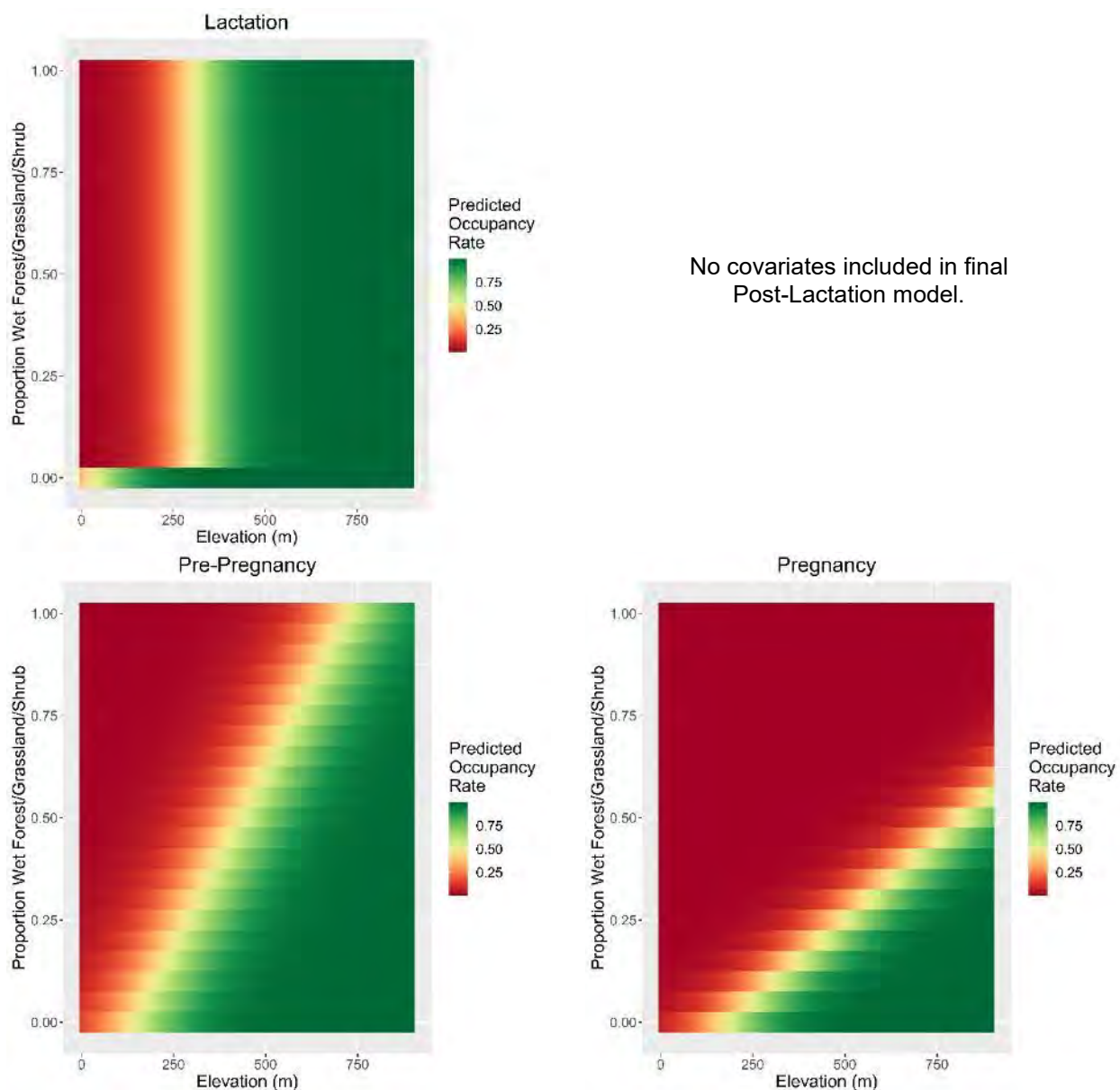**Figure 12. Predicted occupancy by season as a function of elevation (meters [m]) and the proportion of wet forest/grassland/shrub land cover. Note that the Lactation season model contains a classification variable for the proportion of wet forest/grassland/shrub land cover that takes a value of zero if no wet category land cover is present in a grid cell and a value of one if any wet category land cover is present in a grid cell.**

Cyclical Changes in Occupancy

The proportion of operating detectors with any detections was calculated by Julian day and survey year (Figure 13) and the 5-day moving average of daily proportions was calculated by Julian day across survey years (Figure 14). See Appendix C for plots of detections by Julian day and survey year, which exhibit annual fluctuations in detections across years. Daily bat detection across sites was restricted to the smallest proportion of sites during the pre-pregnancy season (Figure 14). This was followed by a gradual increase in detections during the pregnancy season, then a rapid increase during the lactation season followed by a rapid decline during post-lactation (Figures 13 and 14). The peak period of detections during lactation and post-lactation also coincided with a more widespread distribution across Oahu, compared to the more restricted range (based on detections) observed during the pre-pregnancy season.
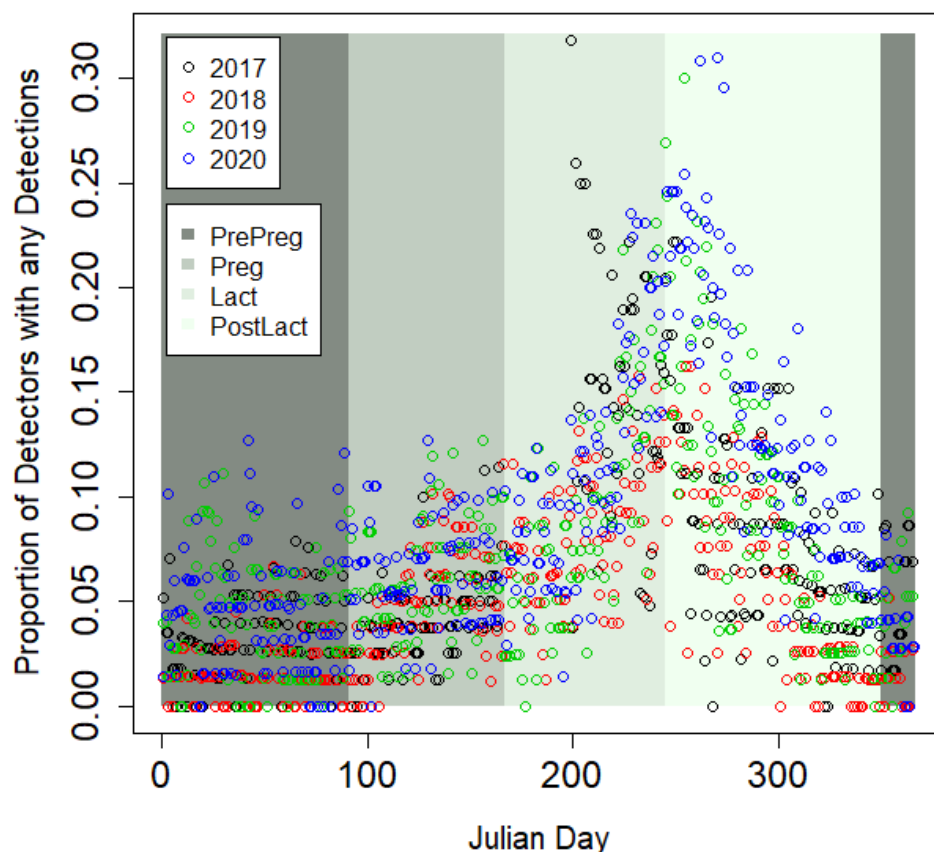

Figure 13. Proportions of detectors with detections by survey year and Julian day.
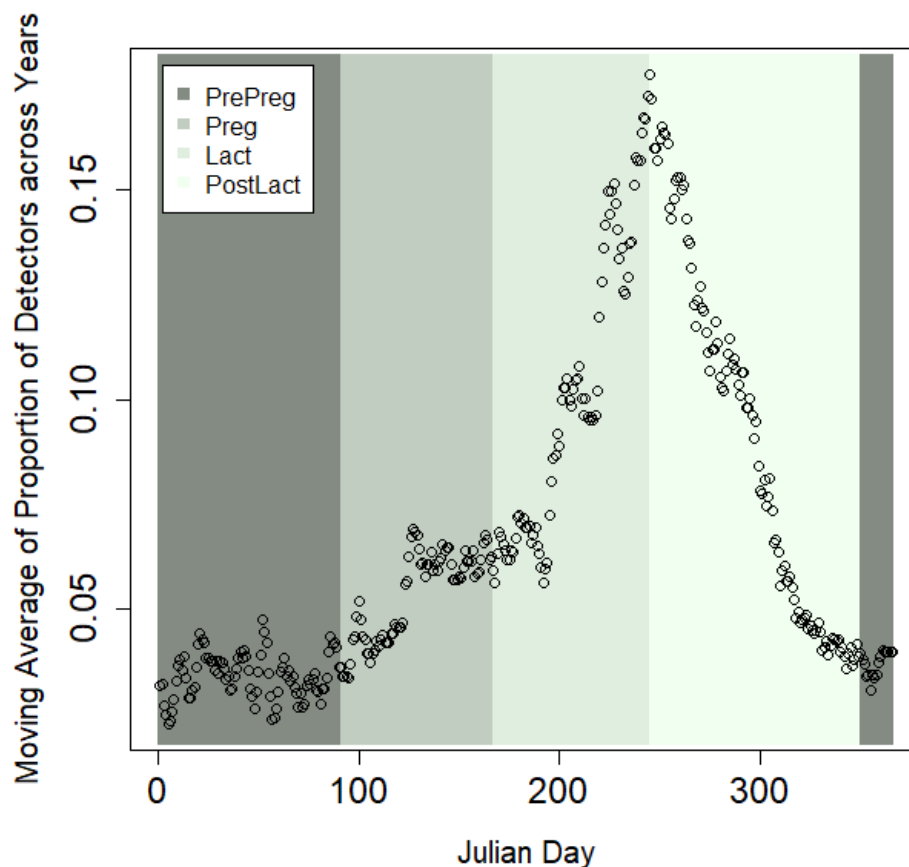
Figure 14. Five-day moving average of the proportion of detectors with detections across survey years by Julian day.

Power Analysis

The results of the power analysis (Table 11) indicate that the power to detect a 10% trend in occupancy over 10 years during the lactation season achieves power of 0.756 or more with as few as 20 sites, and exceeds 0.9 with 40 or more detectors. To detect a 15% annual trend over 10 years, monitoring as few as 20 detectors results in power exceeding 0.9.

Table 11. Power to detect trends in lactation season occupancy of 10% and 15% annually over 10 years.

	10 years	
Number of sites	**Power to detect a 10% annual trend**	**Power to detect a 15% annual trend**
20	0.756	0.932
40	0.916	1
60	0.976	1
80	0.996	1

DISCUSSION

For each of the seasons, occupancy across years was modeled from nightly detections in a sample of 86 selected grid cells. The dynamic occupancy model for correlated detections (Hines et al. 2014) was applied to account for correlation among detections recorded in subsequent nights. In addition to the inclusion of more data, the results reported here differ slightly from the results in previous reports due to changes in the covariate model selection process and changes in the occupancy model, as compared to preliminary reports from the prior years of the study. In this final analysis, a Bayesian modeling approach was used to model trend in occupancy independently by season, as defined above. The probability that a site is occupied in a given year depends on its occupancy state during the same season in the previous year, a practical consideration for a species that potentially occupies different spatial areas throughout the reproductive seasons.

As observed by Menard (2001) and Gorresen et al. (2013), occupancy rates varied by season, with the highest occupancy estimates observed in the lactation and post-lactation seasons and the lowest occupancy rates observed during the pre-pregnancy and pregnancy seasons. Bat occurrence (as indicated by the proportion of detectors with detections) expanded spatially over the pregnancy and lactation seasons, peaked near the beginning of the post-lactation season, and then contracted through the remainder of the post-lactation season to its most spatially restricted period during the pre-pregnancy season (Figures 13 and 14). Occupancy rates exhibited slight but significant increasing trends in both mean and net proportional trends during the pregnancy season (Table 8), while occupancy estimates during the other seasons had upward trajectories over the Study Period (Figure 9), but were not significant (Tables 5–7). This result may change with additional data and increased power to detect significant trends. Given the consistency in results across seasons and years, we infer that the HAHOBA occupancy rate for Oahu was stable to slightly increasing over the Study Period.

Relationships between habitat covariates and occupancy rates were examined by season. No habitat covariates were identified as significant predictors of site occupancy during the post-lactation season, a period when the HAHOBA population appears most dispersed across Oahu and occupancy rates are highest. The broader distribution and increased occupancy rates during this period could be indicative of the dispersal of young-of-the-year bats recently added to the population, versus a broader distribution of adult bats. Effects of elevation were positive for all seasons incorporating site-level covariates in the occupancy model (lactation, pre-pregnancy, and pregnancy), with the effects similar in magnitude among the three seasons (Tables 5, 7, and 8). The proportion of wet forest/grassland/shrub land cover was negatively associated with occupancy during the lactation season, and this negative effect was increasingly pronounced in the pre-pregnancy and pregnancy seasons. Mean monthly Oahu precipitation measured at weather stations between 1920 and 2012 ranged from 5.4 to 6.7 in (13.7 to 17.0 cm) per month from November through April, and from 3.1 to 4.6 in (7.9 to 11.7 cm) per month from May through October (Giambelluca et al. 2013), defining distinct wet and dry periods on Oahu. Predicted HAHOBA occupancy across Oahu (Figure 11) suggests that the drier mid-elevation areas are more consistently occupied throughout the year, while the leeward and more arid side of the island

is preferred during the rainy season occurring principally during the pre-pregnancy season. Therefore, the HAHOBA distribution is most contracted during the wet period, when dry or mesic habitats appear to be preferred over wet habitats.

The U2 microphone yielded higher detection rates than the U1 microphone for every season except the lactation season, when the U1 microphone performed slightly better. The apparent higher detection rate for the U1 microphone during the lactation season is not readily explainable; however, accounting for this difference in the modeling approach is still important and ameliorates the concern that trends in occupancy may have resulted from the change in microphones.

Detection counts examined over time indicate some potential effects of external factors (Appendix C). Daily detections never exceeded 34 at Site-095 until late-summer of 2021 (Appendix C18), when daily detections numbered in the hundreds off and on for over a month. It was noted that invasive vegetation had been cut and removed at this site near the time of the spike in bat activity, suggesting that bat foraging habitat may have improved as a result of the vegetation treatment.

This study and modeling exercise examined main effects of site-level land cover covariates on occupancy rates and acoustic detector microphone models on detection rates independently by season to explore annual trends in occupancy and seasonal distribution of HAHOBA on Oahu. However, this 4-year data set of daily HAHOBA detections also provides a rich basis for additional modeling. Future work could include adding temporal covariates for detection modeling such as Julian date, month, and moon phase cycles. We did not account for environmental variables such as rainfall and temperature data because these data were not available at the site level. However, island-wide means of environmental covariates might provide useful information for modeling annual fluctuations in occupancy rates. Additionally, detection rates could be modeled as a function of habitat covariates to account for differences in echolocation activity in forested vs. non-forested sites (Gorresen et al. 2013). An occupancy model could be developed across all reproductive seasons with extinction and colonization parameters modeled as a function of season, year, and/or habitat covariates. A multistate occupancy analysis (Gorresen et al. 2018) to identify factors associated with high-use areas could provide additional information on habitat selection. Interactions and nonlinear relationships among covariates could also be examined.

A power analysis was conducted to assess the sample size of detectors needed to detect 10% or 15% annual trends in lactation-season occupancy rates over a 10-year period. We found that a sample of at least 30 sites was needed to detect a 10% increase in occupancy, and a sample of 20 detectors would be sufficient to detect a 15% increase in occupancy over 10 years. This prospective power analysis indicates that changes in occupancy could be detected with reasonable power for smaller samples of detectors than we have applied in this study. A fifth year of field data are being collected for a subsample of 40 of the 86 detectors reported on herein. This additional data will be used in an updated analysis to assess a 5-year trend in occupancy on Oahu, the minimum time span considered for assessing population stability in the USFWS' Recovery Plan for the Hawaiian Hoary Bat (USFWS 1998). We would suggest that these smaller samples would provide the best basis for inference if spatial balance and the probabilistic

selection process used in this study were maintained so that the sampled population matches the target population as closely as possible.

REFERENCES

Gelman, A., Carlin, J. B., Stern, H. S., Dunson, D. B., Vehtari, A. and Rubin, D. B., 2013. Bayesian data analysis. CRC press.

Giambelluca, T. W., Q. Chen, A. G. Frazier, J. P. Price, Y. L. Chen, P. S. Chu, J. K. Eischeid, and D. M. Delparte, 2013: Online Rainfall Atlas of Hawai'i. Bull. Amer. Meteor. Soc. 94, 313-316, doi: 10.1175/BAMS-D-11-00228.1. http://rainfall.geography.hawaii.edu/downloads.html

Gorresen, P. M., Brinck, K. W., DeLisle, M. A., Montoya-Aiona, K., Pinzari, C.A., Bonaccorso, F. J. 2018 Multi-state occupancy models of foraging habitat use by the Hawaiian hoary bat (*Lasiurus cinereus semotus*). PLoS ONE 13(10): e0205150. https://doi.org/10.1371/journal.pone.0205150 .

Gorresen, M. P., F. J. Bonaccorso, C. A. Pinzari, C. M. Todd, K. Montoya-Aiona, and K. Brinck. 2013. A Five-Year Study of Hawaiian Hoary Bat (*Lasiurus cinereus Semotus*) Occu Pancy on the Island of Hawai`i. Technical Report HCSU-041. Hawai`i Cooperative Studies Unit. 2 U.S. Geological Survey, Pacific Island Ecosystems Research Center, Kīlauea Field Station. July, 2013. Available online: https://hilo.hawaii.edu/hcsu/documents/TR41_Gorresen_Bat_occupancy.pdf

Hines, J. E., J. D. Nichols, and C. J. A. 2014. Multiseason Occupancy Models for Correlated Replicate Surveys. Methods in Ecology and Evolution 5: 583-591 pp. doi: 10.1111/2041-210X.12186. Available online: https://besjournals.onlinelibrary.wiley.com/doi/pdf/10.1111/2041-210X.12186

LANDFIRE. 2017. Existing Vegetation Type Layer. Landscape Fire and Resource Management Planning Tools Project (LANDFIRE). Department of the Interior (DOI) US Geological Survey (USGS). Last modified February 2017. Available online: http://landfire.cr.usgs.gov/viewer/

MacKenzie, D. I. 2006. Modeling the Probability of Resource Use: The Effect of, and Dealing with, Detecting a Species Imperfectly. Journal of Wildlife Management 70(2): 367-374. doi: 10.2193/0022-541x(2006)70[367:mtporu]2.0.co;2.

MacKenzie, D. I., J. D. Nichols, J. A. Royle, K. H. Pollock, L. L. Bailey, and J. E. Hines. 2006. Occupancy Estimation and Modeling: Inferring Patterns and Dynamics of Species Occurrence. Academic Press, Elsevier, Burlington, Massachusetts.

Menard, T. 2001. Activity Patterns of the Hawaiian Hoary Bat (*Lasiurus cinereus Semotus*) in Relation to Reproductive Time Periods. MSc Thesis. University of Hawaii. Available online: https://www. opeapea.org/paper-blog/2019/2/2/Activity%20patterns%20of%20the%20Hawaiian%20hoary%20 bat%20(Lasiurus%20cinereus%20semotus)%20in%20relation%20to%20reproductive%20time%2 0periods.%20MSc%20Thesis,%20University%20of%20Hawaii.

Mitchell, T. J.; Beauchamp, J. J. 1988. Bayesian Variable Selection in Linear Regression. Journal of the American Statistical Association. 83(404):1023–1032.

National Geographic Society (National Geographic). 2020. World Maps. Digital topographic map. PDF topographic map quads. Accessed January 2020. Available online: http://www.natgeomaps. com/trail-maps/pdf-quads

Pinzari, C., K. Montoya-Aiona, D. Gross, and K. Courtot. 2021. Hawaiian Hoary Bat Acoustic Surveys on Marine Corps Base Hawaii, 2019-2021. DOI: 10.5066/P9L9HY6D. Report number: TR-100 University of Hawaii at Hilo. Available online: https://www.researchgate.net/publication/356223824_Hawaiian_hoary_bat_acoustic_surveys_on_Marine_Corps_Base_Hawaii_2019-2021

Plummer, M. 2019. rjags: Bayesian Graphical Models using MCMC. R package version 4-10. https://CRAN.R-project.org/package=rjags.

R Development Core Team. 2021. R: A Language and Environment for Statistical Computing. R Foundation for Statistical Computing, Vienna, Austria. Information online: http://www.R-project.org/

Starcevich, L. A., J. Thompson, T. Rintz, E. Adamczyk, and D. Solick. 2019. Oahu Hawaiian Hoary Bat Occupancy and Distribution Study: Project Update and First-Year Analysis. Prepared for Hawaii Endangered Species Research Committee. Western Ecosystems Technology, Inc. Corvallis, OR.

Starcevich, L. A., J. Thompson, T. Rintz, E. Adamczyk, M. Martin, and D. Solick. 2020. Oahu Hawaiian Hoary Bat Occupancy and Distribution Study: Project Update and Second Year Analysis. Prepared for Hawaii Endangered Species Research Committee. Western Ecosystems Technology, Inc. Corvallis, OR.

Stevens, D. L., Jr. and A. R. Olsen. 2003. Variance Estimation for Spatially Balanced Samples of Environmental Resources. Environmetrics 14(6): 593-610 pp. doi: 10.1002/env.606. Available online: https://onlinelibrary.wiley.com/doi/abs/10.1002/env.606

Stevens, D. L., Jr. and A. R. Olsen. 2004. Spatially Balanced Sampling of Natural Resources. Journal of the American Statistical Association 99(465): 262-278. doi: 10.1198/016214504000000250.

Thompson, J., and L.A. Starcevich. 2021. Oahu Hawaiian Hoary Bat Occupancy and Distribution Study: Project Update and Third-Year Analysis. Prepared for Hawaii Endangered Species Research Committee. Western Ecosystems Technology, Inc. Corvallis, OR.

US Census Bureau. 2019. 2010 Census - Block Maps. Last update: March 14, 2019. Accessed July 2022. Available online: https://www.census.gov/geographies/reference-maps/2010/geo/_2010-census-block-maps.html

US Geological Survey (USGS). 2017. USGS National Elevation Dataset (NED). State of North Dakota, State Water Commission. Last updated February 27, 2019. Available online: https://catalog.data.gov/dataset/usgs-national-elevation-dataset-ned

US Fish and Wildlife Service (USFWS). 1998. Recovery Plan for the Hawaiian Hoary Bat. U.S. Fish and Wildlife Service, Portland, OR. 50 pp. Available online: https://ecos.fws.gov/docs/recovery_plans/1998/980511b.pdf

Wildlife Acoustics, Inc. 2019. Kaleidoscope Pro® Version 5.1.0. (Acoustic analysis computer software). Wildlife Acoustics, Maynard, Massachusetts. Information online: www.wildlifeacoustics.com

Wright, W. J., K. M. Irvine, and T. J. Rodhouse. 2016. A Goodness-of-Fit Test for Occupancy Models with Correlated within-Season Revisits. Ecology and Evolution 6(15): 5404-5415 pp. doi: 10.1002/ece3.2292. Available online: https://onlinelibrary.wiley.com/doi/full/10.1002/ece3.2292